

Diagnostics for Light Sources

Introduction

Diagnostics Systems & Related Measurements

Electron Beam Position Monitors

Photon Beam Position Monitors

Current Monitors

Synchrotron Light Monitors

V. Schlott (PSI)

Acknowledgements

- ... to be able to present a state-of-the-art overview of light source diagnostics, I have been relying on the outstanding work of many colleagues from various synchrotron radiation facilities
- ... this presentation is far from being complete ! It tries to give an overview of light source diagnostics with a number of – hopefully instructive – examples and (latest) measurements
- ... for their support in discussing the topics, which are presented, and for the provision of information material and measurement results, I would like to explicitly thank the following colleagues...:

Andreas Streun (PSI)

Michael Böge (PSI)

Thomas Schilcher (PSI)

Boris Keil (PSI)

Andreas Lüdeke (PSI)

Thomas Wehrli (PSI)

Juraj Krempaski (PSI)

Gero Kube (DESY)

Ake Andersson (MaxLab)

Günther Rehm (DIAMOND)

Jean-Claude Denard (SOLEIL)

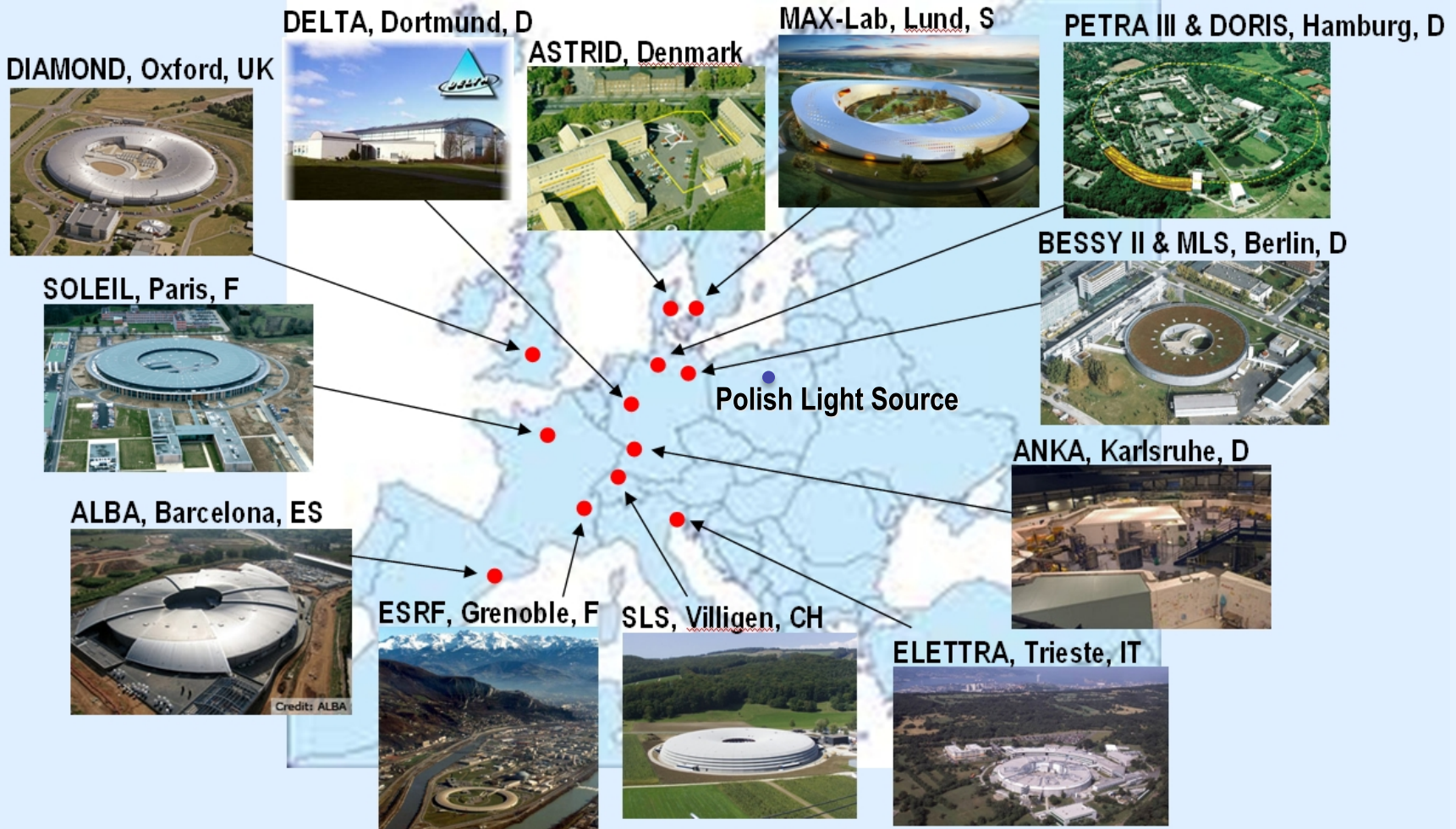
Peter Kuske (BESSY)

Karsten Holldack (BESSY)

Mario Ferianis (ELETTRA)

and many more...!!!

3rd Generation Synchrotron Radiation User Facilities in Europe



3rd Generation Light Source User Facilities: SLS Beamlines (2010)

Number of Beamlines: several tens

Photon Energies: THz – > 100 keV

Flux: $\leq 10^{13}$ ph / (s 0.1%BW)

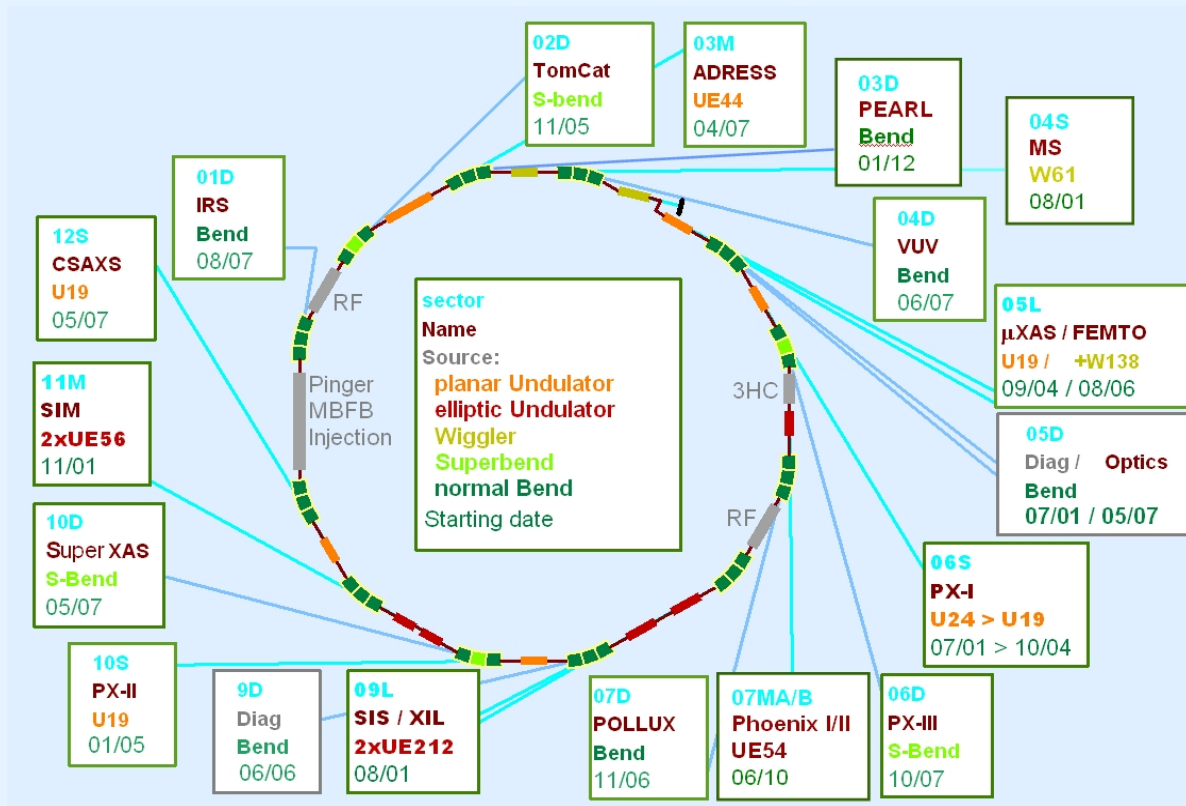
Brilliance: $\leq 10^{21}$ ph / (s mm² mrad² 0.1%BW)

Photon Spot Sizes: sub- μ m – few 100 μ m

Photon Beam Stability: $\sigma / 10$ ($\geq 1 \mu$ m)

Photon Pulse Widths: few ps – 300 ps

~ 100 fs (FEMTO-slicing)



Typical Layout & Accelerator Parameters of a 3rd Generation Light Source

Pre-Injector LINAC Parameters

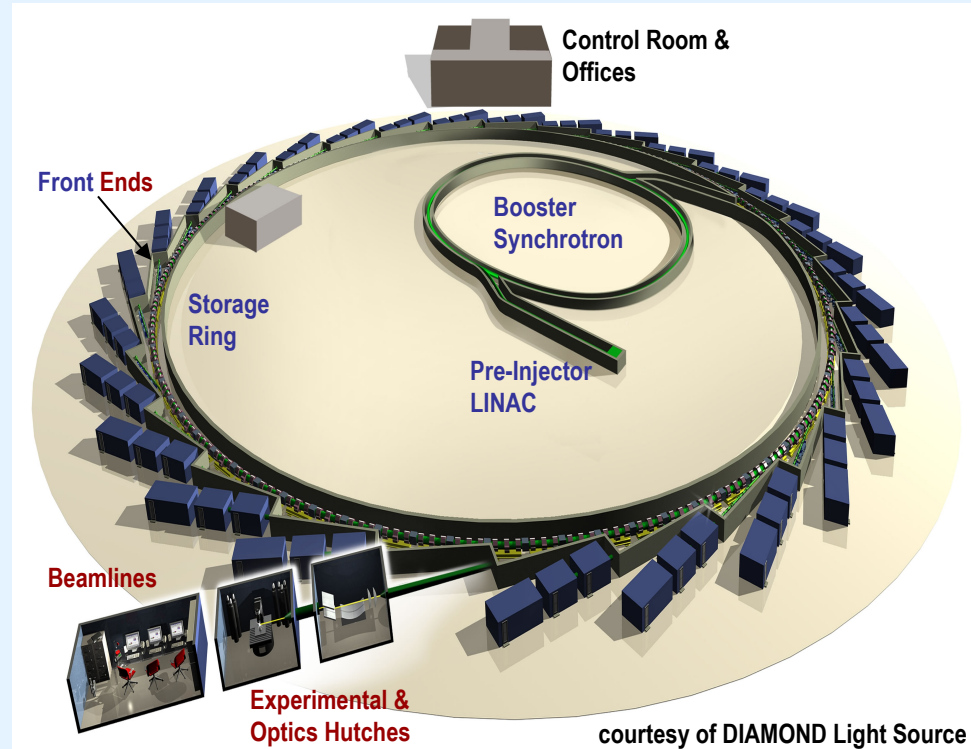
Operation Modes:	single bunch / bunch train
Typ. Energy:	100 – few MeV
Max. Charge:	$\leq 2 \text{ nC}$ / $\leq 5 \text{ nC}$
$\Delta E/E$:	$< 0.5\%$ (0.2 %)
Energy Stability:	$< 0.1\%$ (0.1%)
Timing Jitter:	$< 100 \text{ ps}$ (10 ps)
Typ. Emittance:	$< 50 \text{ mm mrad}$
Rep.-Rate:	$< 10 \text{ Hz}$

Booster Synchrotron Parameters

Energy Ramp:	few 100 MeV – few GeV
Ramp Times:	$\sim 100 \text{ ms}$
Design Current:	$\leq 3 \text{ mA}$
Design Emittance:	$< 250 \text{ nm mrad}$
Efficiency:	$\sim 80\%$
Rep.-Rate:	$< 10 \text{ Hz}$

Storage Ring Parameters (European Light Sources)

Electron Energies:	105 MeV – 6 GeV	Horiz. Emittances:	1 – 100 nm rad	Filling Pattern:	single & multiple bunches camshaft to uniform
Beam Currents:	100 pA – 500 mA	Coupling:	$< 0.1 - 1\%$	RF Frequencies:	100 – 500 MHz
Life Times:	10 – 75 h	Vert. Emittances:	$\geq 3 \text{ pm rad}$	Bunch Spacings:	10 – 2 ns
	top-up operation	Horiz. Beam Sizes:	few tens of μm	Bunch Lengths:	few ps – 300 ps
MTBF / Beam Loss:	$< 175 \text{ h}$	Vert. Beam Sizes:	few μm	Orbit Stability:	$< 1 \mu\text{m}$ (MTF to 200 Hz)
Circumferences:	48 – 2300 m	Horiz. Divergence:	few tens of μrad		
Revolution Frequ.:	6.25 – 0.130 MHz	Vert. Divergence:	few μrad		



Diagnostics Requirements for 3rd Generation Light Sources

the **key parameter** to be optimized in 3rd generation light sources is the **spectral brilliance**

$$B \propto \frac{N_{photons}}{\sigma_x \sigma_x \sigma_y \sigma_y} \propto \frac{I_{beam}}{\varepsilon_x \varepsilon_y} \left[\frac{\text{Number of Photons}}{mm^2 mrad^2 0.1\% \text{ bandwidth}} \right]$$

- **high beam current** - ideally „top-up“ operation
highly efficient, low loss injector chain
- **small beam emittances** - ideally low coupling (< 0.1%)
measurement of small beam sizes with high resolution SR monitors
- **high beam stability** - ideally „top-up“ operation with fast and slow orbit feedbacks
high resolution electron and photon BPM systems

Overview of Diagnostics Devices for 3rd Generation Light Sources

Beam Position Monitors:

- Button BPMs: x_k, y_k, I_k (k = BPM index)
- commissioning & injection studies
 - orbit correction & FOFB
 - tunes and chromaticity
 - local and global coupling / resonances

Bunch Charge & Current Monitors:

- ICT / BCM in LINAC and TLs
- transmission and injection efficiency
- MPCT in booster synchrotron
- beam current and transmission on the ramp
- DCCT / PCT in storage ring
- injection efficiency and stored current
 - beam lifetime

Transverse Profile Monitors:

- OTR and scintillator screens
- beam profiles, emittance & $\Delta E/E$ in LINAC & TLs
 - injection matching in booster & storage ring
- synchrotron radiation monitors
- beam size, emittance & coupling

Longitudinal Profile Monitors:

- Wall Current Monitors, FCTs
- bunch pattern in LINAC & TLs
 - bunch purity in LINAC & TLs
- Streak Camera
- bunch length / lengthening in storage ring
 - longitudinal instabilities in storage ring
- Fast Diodes / PMs
- bunch pattern / bunch pattern FB in storage ring
 - bunch purity (in photon counting mode)

Beam Loss Monitors & Scrapers:

- local and global beam loss (low gap undulators)
- lifetime
- dynamic aperture studies
- limitation of storage ring aperture

Photon Beam Monitors:

- photon beam position (undulator gap compensation)
- absolute orbit reference & long term stability
- FOFB „out of loop monitors“
- more potential...!

Beam Position Monitors: Modes of Operation & Specifications

injection & commissioning mode:

- x_k, y_k and I_k upon injection trigger ($k = \text{BPM index}$)
- data processing & transfer in batches
- position resolution: $< 500 \mu\text{m}$ (rms)
- absolute accuracy: $< 500 \mu\text{m}$ (with respect to quad)
- intensity / charge res.: $\sim 10\%$ / $\geq 50 \text{ pC}$
- dynamic range: $< 0.5 - 5 \text{ mA}$
- current dependency: $< 500 \mu\text{m}$ (within 10dB range)

turn-by-turn mode:

- x_k, y_k for several thousand turns ($k = \text{BPM index}$)
- data processing & transfer in batches
- position resolution: $\sim 1 \mu\text{m}$ (rms)
- absolute accuracy: $< 200 \mu\text{m}$ (with respect to quad)
- measurement bandwidth: $< 1 \text{ MHz}$
- dynamic range: $5 - 100 \text{ mA}$
- current dependency: not critical for BD studies
- drift (8h – 1 month): not critical for BD studies
- reproducibility (bunch pattern): $< 500 \mu\text{m}$

closed orbit correction mode:

- x_k, y_k ($k = \text{BPM index}$)
- measurement rate: few samples per second
- position resolution: $< 0.2 \mu\text{m}$ (rms)
- absolute accuracy (after BBA): $< 1 \mu\text{m}$ (with respect to quad)
- measurement bandwidth: few kHz
- dynamic range: $10 - 100 \text{ mA}$
 $100 - 500 \text{ mA}$
- current dependency: $< 1 \mu\text{m}$ (10 dB range)
- drift (8h – 1 month): $< 1 \mu\text{m}$ / $< 5 \mu\text{m}$
- reproducibility (bunch pattern): $< 1 \mu\text{m}$

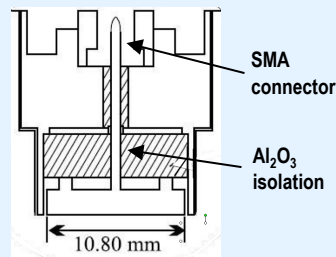
global fast orbit feedback mode:

- x_k, y_k ($k = \text{BPM index}$)
- measurement rate: 10 kSamples per second
- position resolution: $< 0.2 \mu\text{m}$ (rms)
- absolute accuracy (after BBA): $< 1 \mu\text{m}$ (with respect to quad)
- measurement bandwidth: few kHz
- dynamic range: $10 - 100 \text{ mA}$
 $100 - 500 \text{ mA}$
- current dependency: $< 5 \mu\text{m}$ (10 dB range)
- drift (8h – 1 month): $< 1 \mu\text{m}$ / $< 5 \mu\text{m}$
- reproducibility (bunch pattern): $< 1 \mu\text{m}$

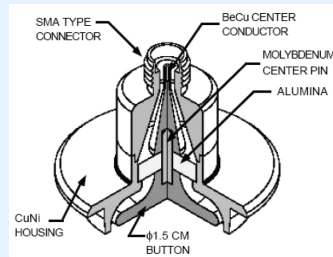
Beam Position Monitors: Signal Considerations for Button Electrodes

Examples of Button Electrodes:

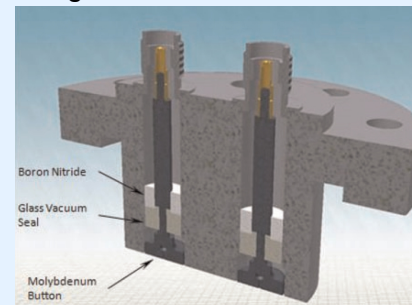
Welded ESRF / DELTA Button



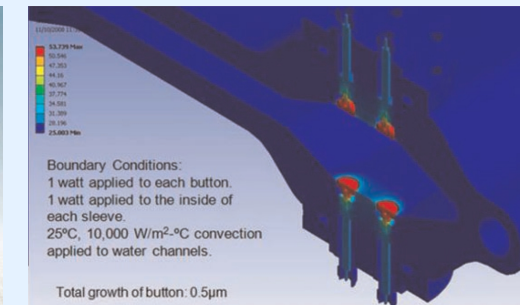
HERA Button



Flanged NSLS-II Button



Heat Load Simulation for NSLS-II Button



Induced Voltage on Electrode

- with a = button radius (typ. 5 – 10 mm)
- b = BPM chamber radius (typ. 15 - 20 mm)
- $\beta \approx 1$
- c = speed of light
- $R = 50 \Omega$ (termination, dominated by cable)
- f = processing frequency (typ. ≤ 500 MHz)

$$V_{button} = \frac{\pi a^2}{2\pi b} \cdot \frac{R}{\beta c} \cdot \frac{dI}{dt}$$

$$= \frac{2\pi a^2}{b} \cdot \frac{R}{\beta c} \cdot f I_{avg}$$

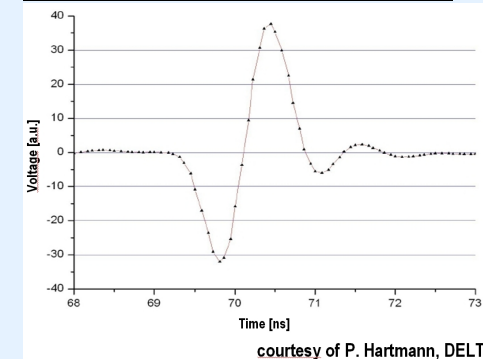
Signal Power for 100 mA Beam:

- with noise power in 1 MHz BW: ~ 114 dBm
- in 10 kHz BW: ~ 134 dBm

$$P_{signal} = \frac{1}{2} \frac{V_{button}^2}{R}$$

$$\approx 0.67 \mu W \approx -32 \text{ dBm}$$

Voltage at Storage Ring Button Electrode



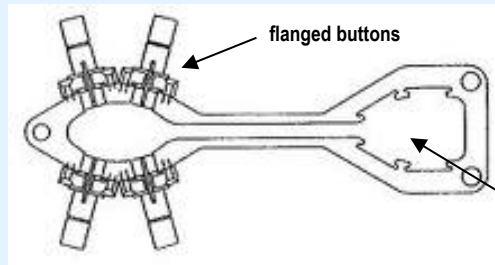
For further reading see e.g.:

- R.E. Schafer, „Beam Position Monitoring“, AIP Conf. Proc. Vol. 212, pp. 26-58 (1989)
- AIP Conf. Proc. 249, vol. 1, 612 (1992)
- S. R. Smith, „Beam Position Monitor Engineering“, SLAC-PUB-7244, July 1996
- P. Forck et al., „Beam Position Monitors“, CAS Beam Diagnostics 2008, 187, CERN-2009-005

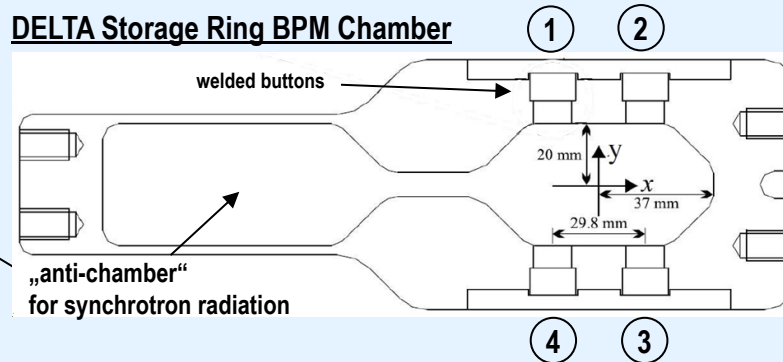
Beam Position Monitors: Storage Ring Chamber Geometries

Examples of Storage Ring BPM Chambers:

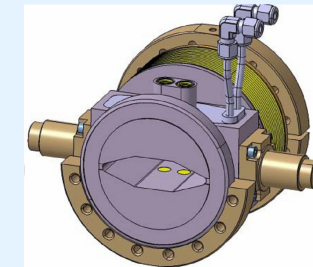
APS Storage Ring BPM Chamber



DELTA Storage Ring BPM Chamber



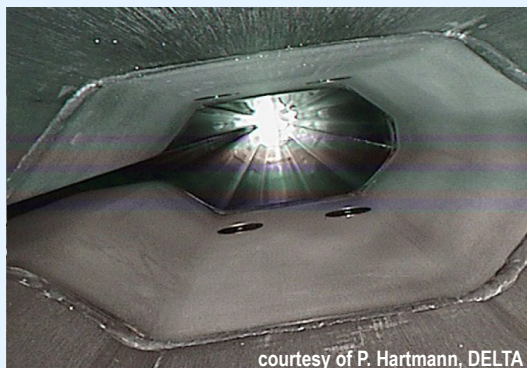
SOLEIL Arc Chamber



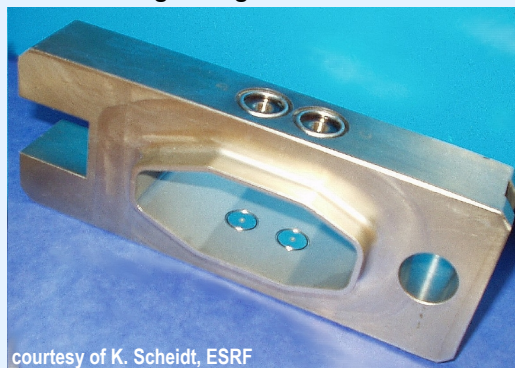
Note...:

- ... due to heat load from synchrotron radiation, button electrodes have been placed outside of the beam plane
- ... BPM chamber is typically a massive SS block, which is welded or flanged to the storage ring vacuum chamber
- ... storage ring vacuum chamber should typically be supported at the locations of the BPM chamber for minimum displacements

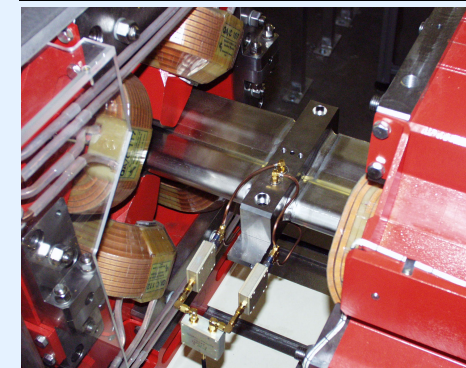
Inside View of DELTA BPM Chamber



ESRF Storage Ring BPM Chamber



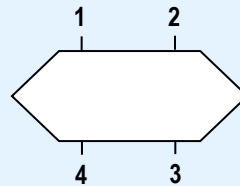
SLS MBF BPM Chamber (with Hybrids)



Light Source BPMs: Position Sensitivity & Non-Linearities

Determination of Horizontal Position:

$$X_{pos} = \frac{1}{S_x} \cdot \frac{(V_1 + V_4) - (V_2 + V_3)}{V_1 + V_2 + V_3 + V_4}$$



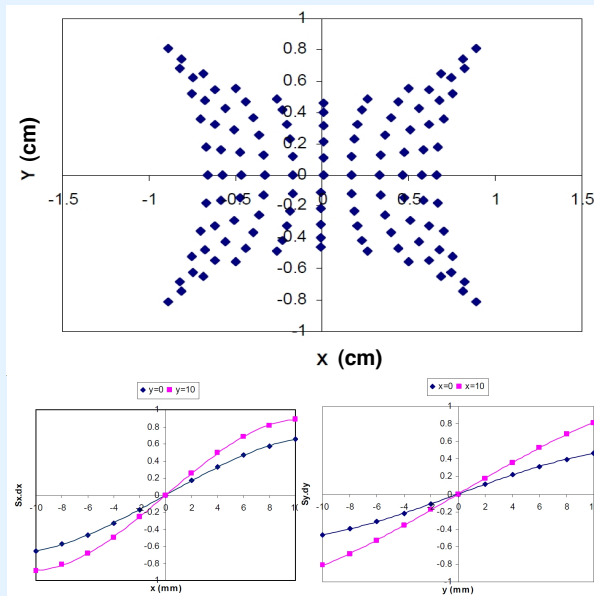
Determination of Vertical Position:

$$Y_{pos} = \frac{1}{S_y} \cdot \frac{(V_1 + V_2) - (V_3 + V_4)}{V_1 + V_2 + V_3 + V_4}$$

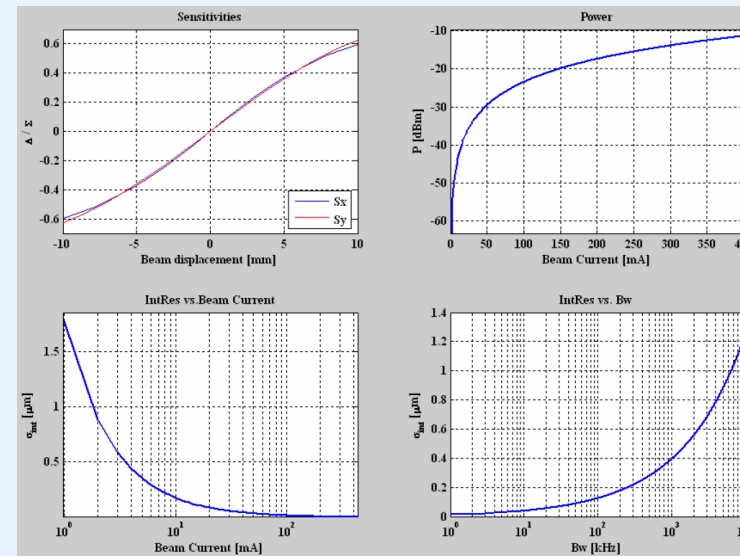
Sensitivity parameters S_x, S_y depend on geometry of vacuum chamber, size and distance between electrodes

- general optimization of geometry is obtained by numerical simulations
- S_x, S_y are typically determined by polynomial fits and given in [% / mm]

SESAME BPM Sensitivity Map (Varnasseri et al., DIPAC 2005)



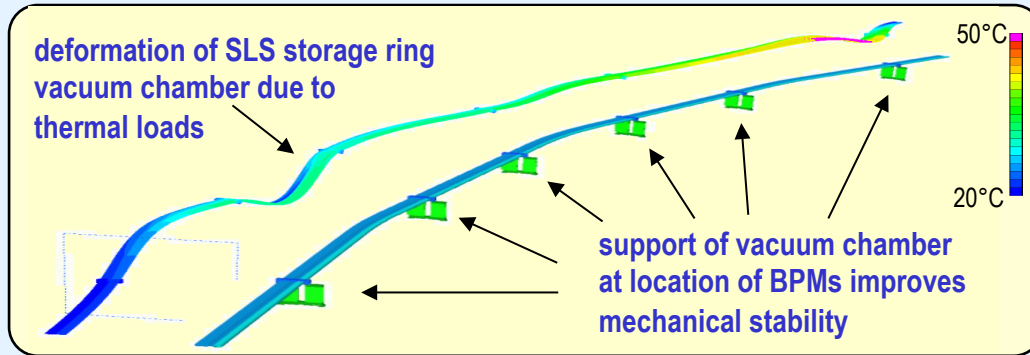
ALBA BPM Simulation Toolbox (Olmos et al., DIPAC 2007)



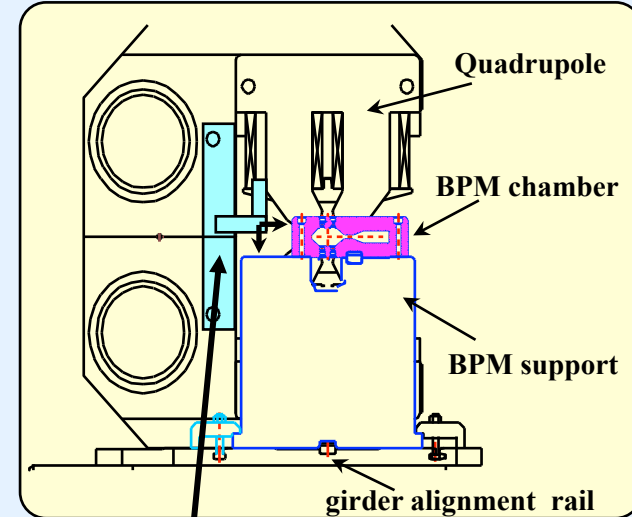
http://www.cells.es/Divisions/Accelerators/RF_Diagnostics/Diagnostics/OrbitPosition/Tools/BPMs_GUI

Storage Ring BPMs: Some Mechanical Considerations & Stability Issues

Thermal Load on SLS Vacuum Chamber due to Synchrotron Radiation



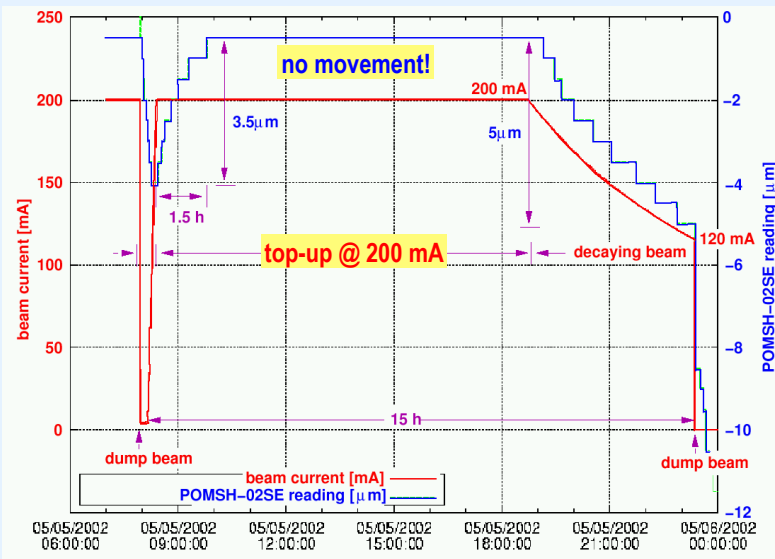
Monitoring Mechanical Movements at SLS



dial gauges equipped with linear encoders (0.1 - 0.5 μm resolution) as sensing devices are attached to adjacent quadrupole magnets

BBA results provide absolute reference positions

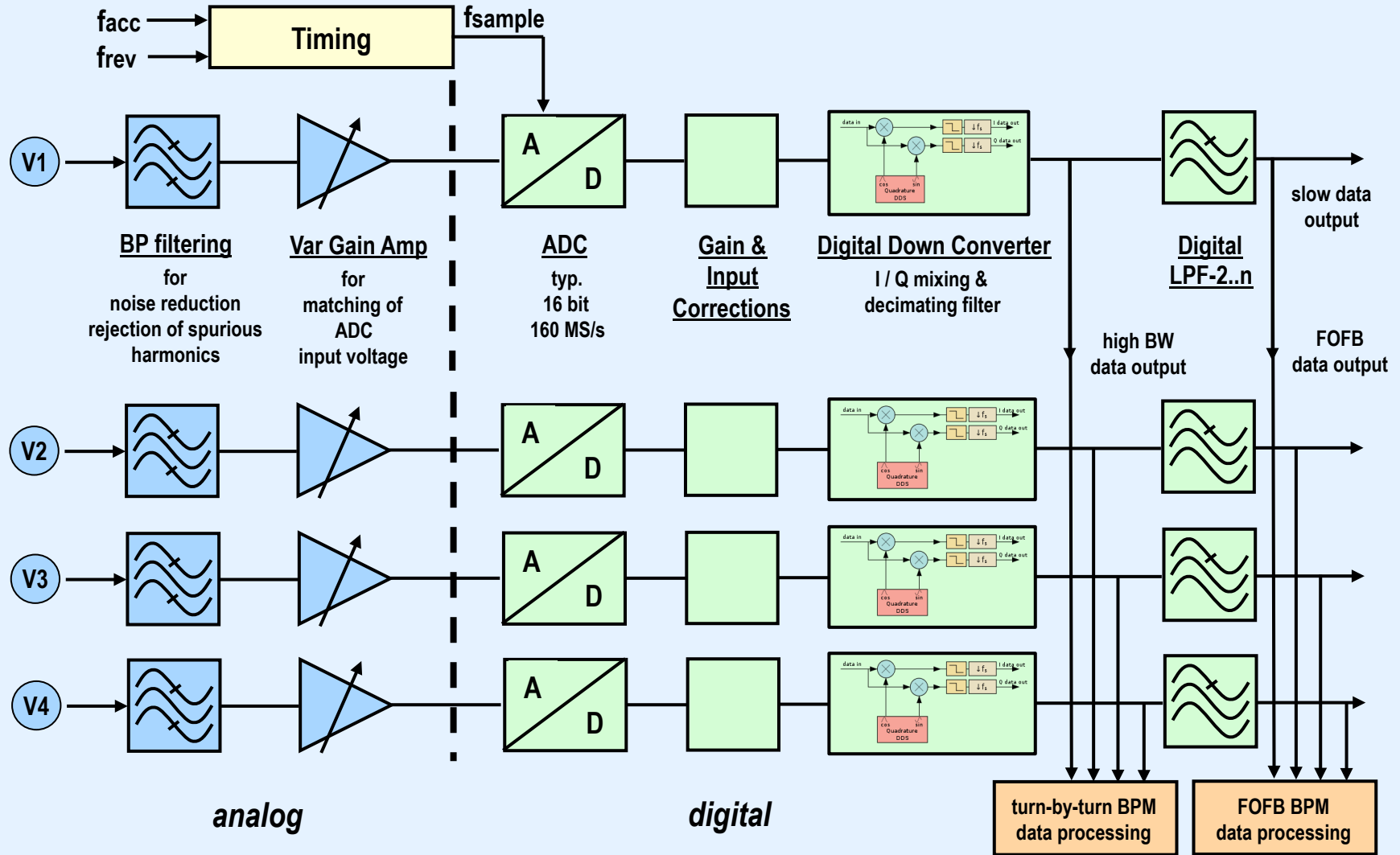
Mechanical Movements of SLS BPM Chambers



Top-Up Operation is the Cure...!!!

- thermal & mechanical stability
- no BPM current dependency

Schematic of Light Source Beam Position Monitor Electronics

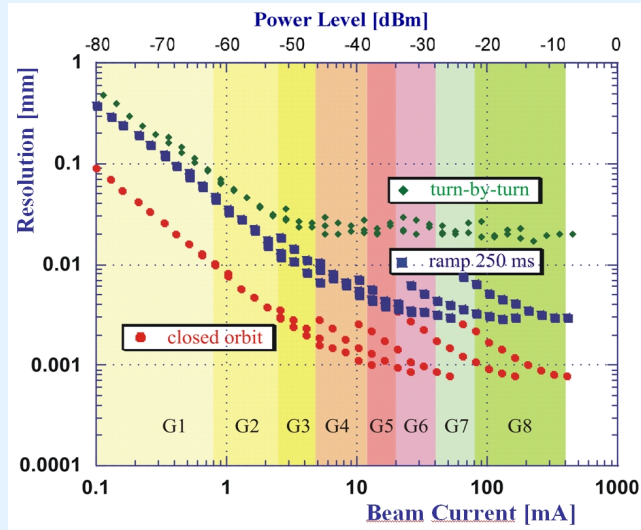


Typical Performances of Light Source Beam Position Monitor Electronics

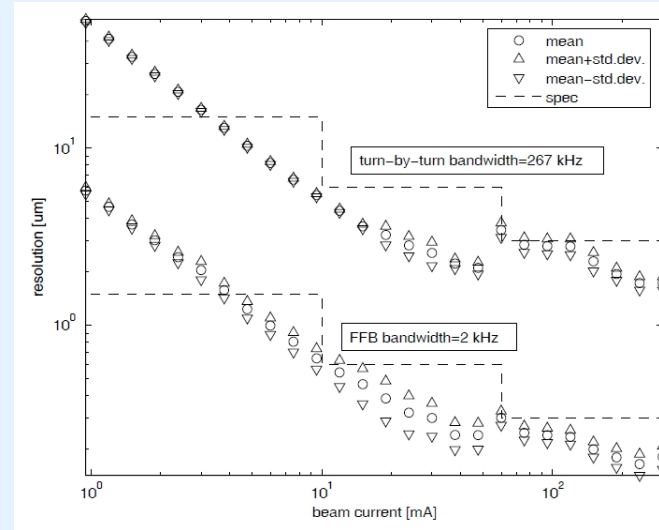
- Digital BPM Systems** provide:
- ... selectable bandwidth of BPM data (turn-by-turn, ramp, FOFB...)
 - ... high resolution, low current dependency, low drift and high reproducibility
 - ... in future direct sampling of BPM pick-up signals should be possible

Examples of Light Source BPM System Performances for Different Operation Modes

SLS DPBM Performance (measurements from 2003)



DIAMOND Libera Performance (G. Rehm et al., DIPAC 2005)

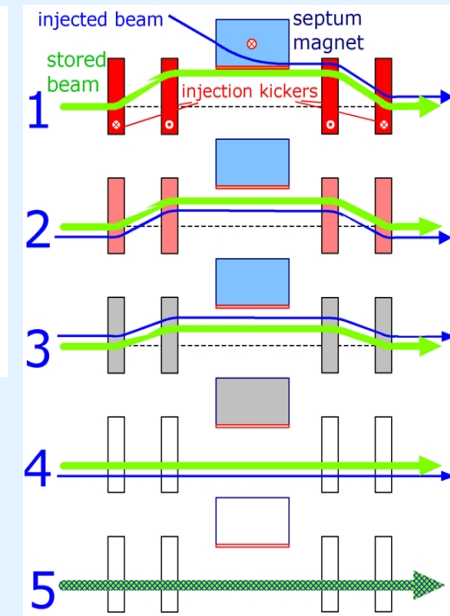
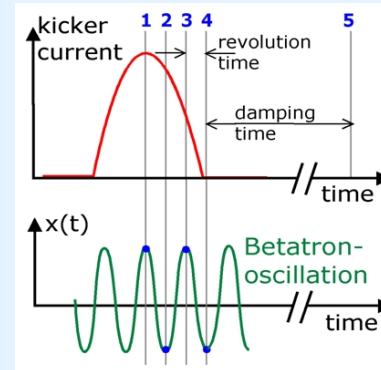


- Some Remarks:**
- ... due to „top-up“ operation, SLS DBPM system is operated at constant gain levels
 - ... position resolution follows the bandwidth restriction ($\sim \sqrt{BW}$ relation)
 - ... next generation DBPM system Libera (Brilliance) provides already improved position resolution

BPM Applications I: Measurement & Optimization of Storage Ring Injection

Pinciple of „4 Kicker Injection“:

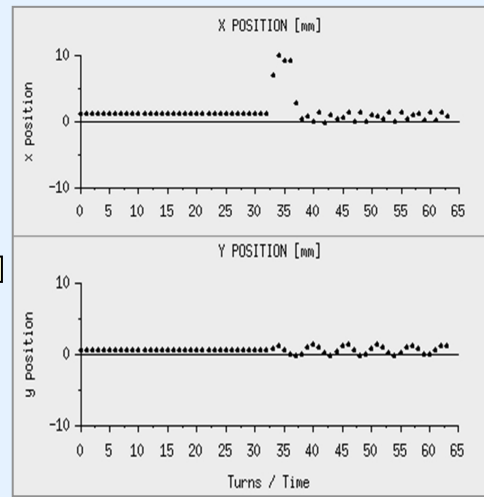
- 1 all 4 kickers „fired“:
the stored beam performs a „closed bump“,
the injected beam enters the storage ring through the septum
- 2/3 all 4 kickers turned off:
the „closed bump“ of the stored beam fades away,
the orbit of the injected beam oscillates around the stored beam
- 4/5 all 4 kickers off:
betatron oscillation of injected beam damps down
→ beam is injected and stored on closed orbit



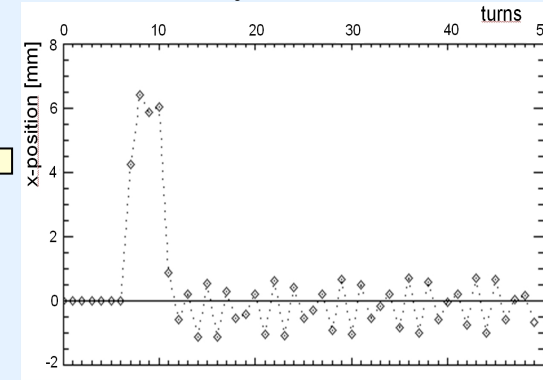
Establishment of Closed Orbit from all BPMs (I, X and Y)



Single BPM Turn-by-Turn Meas. of Injection Kick



Simulation of SLS Injection Kick



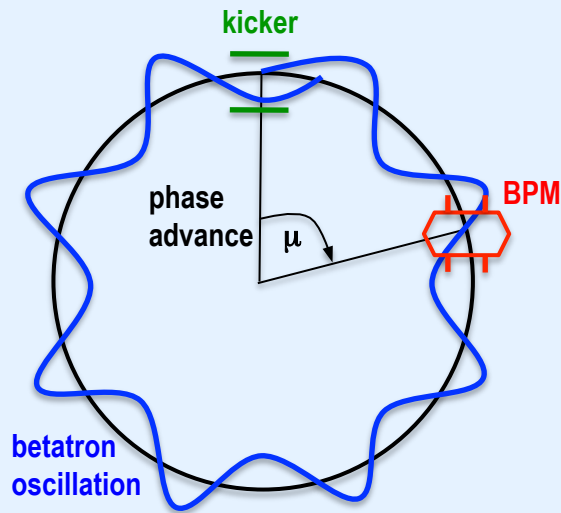
BPM Applications II: Tune Measurement

Principle of Tune Measurement:

- excitation of betatron oscillation by kicker magnet (e.g.: septum, MBF kicker)
- **BPM measures turn-by-turn data** (e.g.: 4096 horizontal & vertical positions)
- FFT on position readings provides integer part of the tune

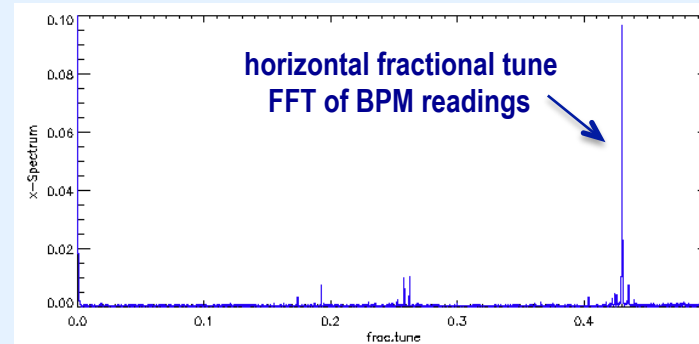
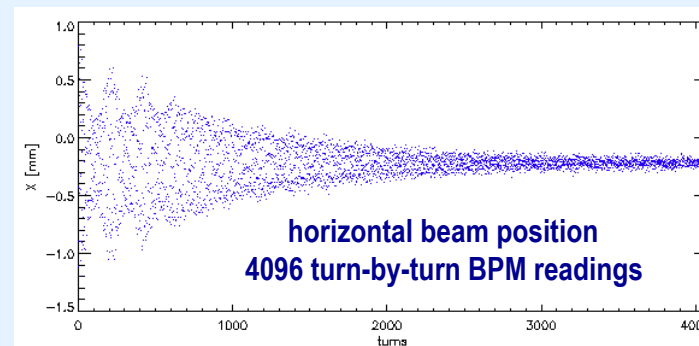
Tune Definition:

betatron phase advance over one turn



$$Q = \frac{1}{2\pi} \oint_C \mu(s) ds$$

$$\Delta x_\beta = \sqrt{\varepsilon\beta} \sin(\mu + \phi_i + 2\pi Qn)$$



BPM Applications III: Chromaticity and Beta Function / Orbit Response

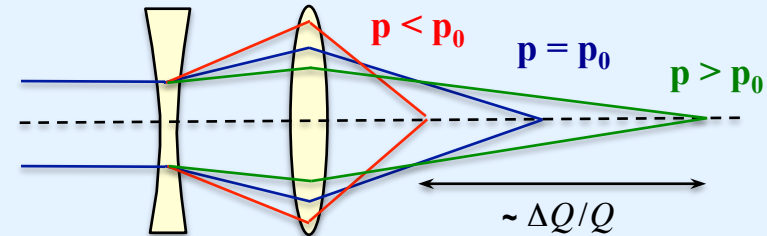
Chromaticity is a momentum-induced tune shift

→ tune spread depends on momentum spread

$$\frac{\Delta Q}{Q} = \xi \frac{\Delta p}{p}$$

Pinciple of Chromaticity Measurement:

- measure tune Q_1
- change $\Delta p/p$ (e.g. RF frequency) and measure tune Q_2
- determine tune shift $\Delta Q = Q_2 - Q_1$



BPMs measure in turn-by-turn mode

β -Function / Orbit Response Measurement Methods

→ determination of **tune shift** induced by quadrupole strength modulation

$$\Delta Q = \frac{1}{4\pi} \int_{s_0}^{s_0+L} \Delta K \beta(s) ds \cong \frac{\Delta K \bar{\beta} L}{4\pi}$$

- each BPM records **position change** induced by **orbit kick** from each corrector
- **orbit response matrix** A_{ij} relates orbit positions & corrector deflections
- fit of β -functions by „linear optics from closed orbit“ (LOCO)

$$\vec{u} = A_{ij} \vec{\theta}$$

$$A_{ij} = \frac{\sqrt{\beta_i \beta_j} \cos(|\mu_i - \mu_j| - \pi Q)}{2 \sin(\pi Q)}$$

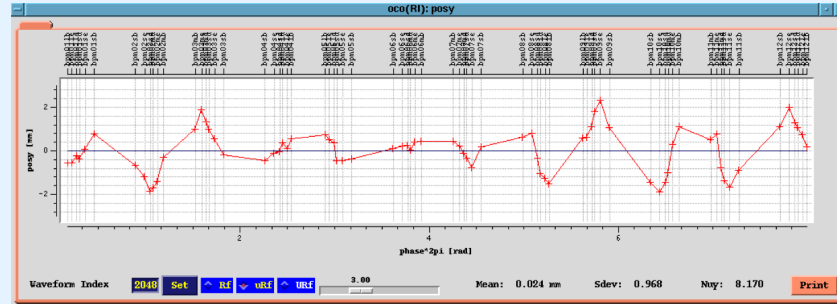
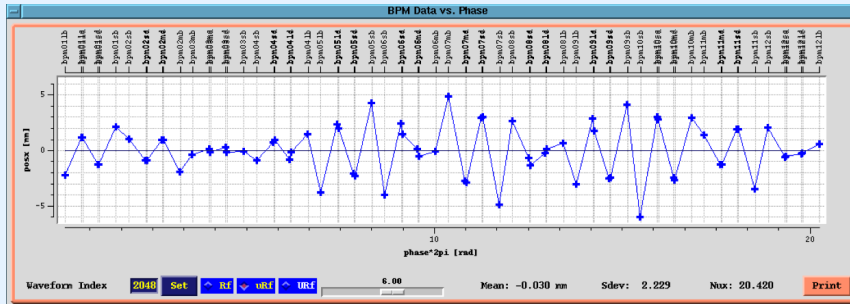
BPM Applications IV: Orbit Correction & Establishment of Golden Orbit

courtesy of Michael Boege, PSI

SLS „bare orbit“ without corrections:

$x_{rms} = 2.3 \text{ mm}, y_{rms} = 1 \text{ mm}$

→ upper limit of sextupole & quadrupole alignment errors of $< 30 \mu\text{m}$

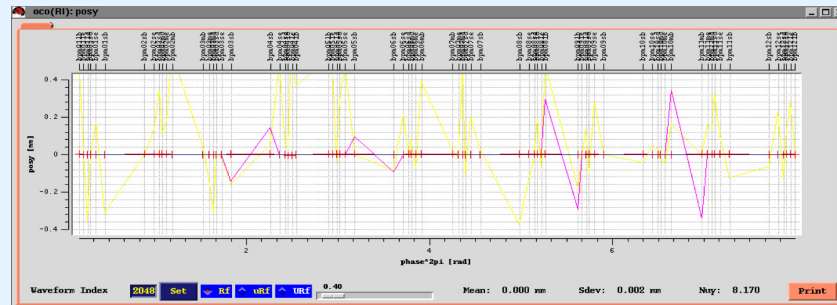
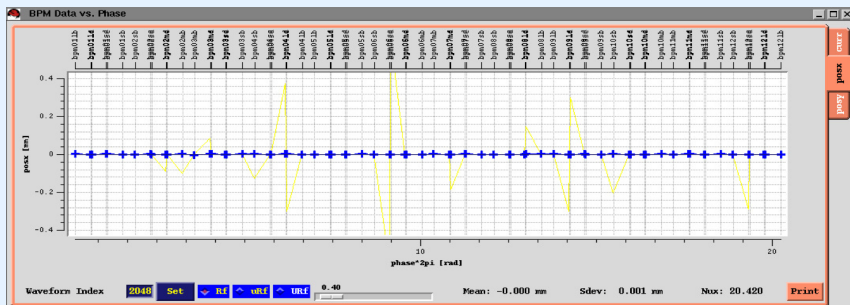


→ global orbit correction is achieved by „single value decomposition“ (SVD) of response matrix A_{ij}

SLS „golden orbit“ after CO correction:

$x_{rms} = 1 \mu\text{m}, y_{rms} = 1 \mu\text{m}$

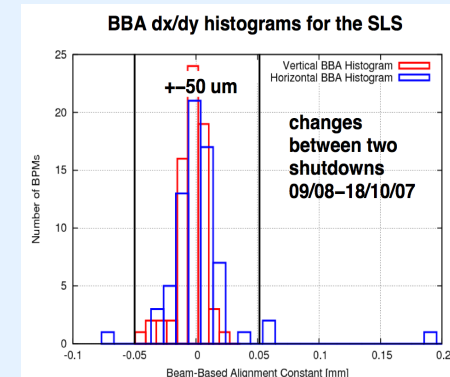
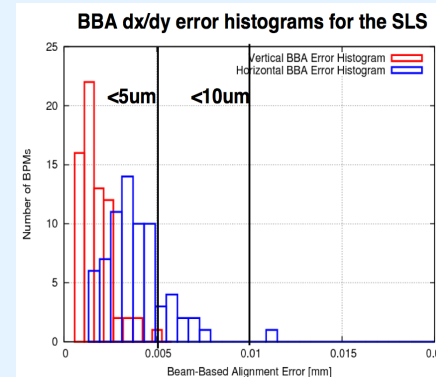
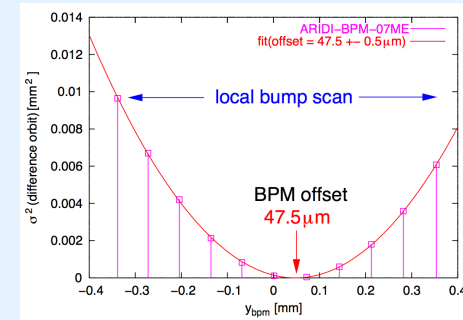
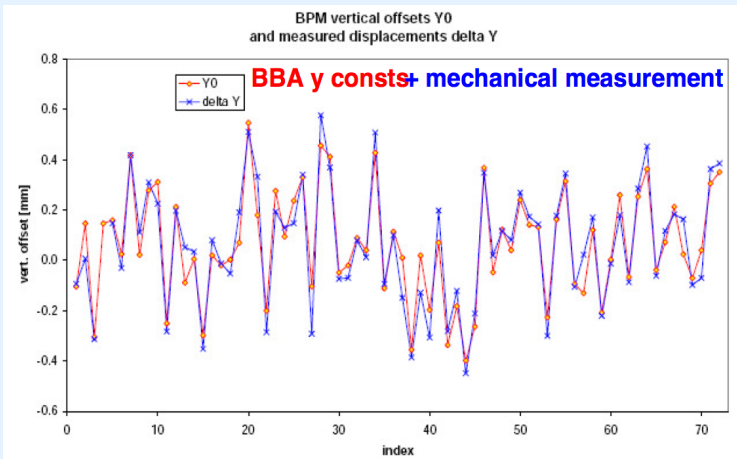
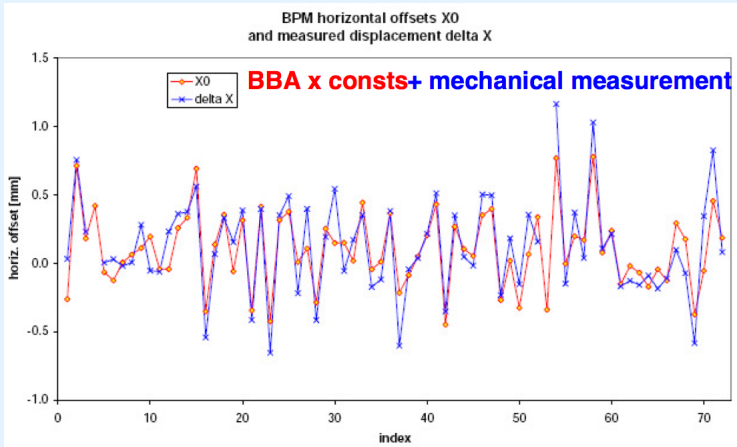
→ each beamline receives its individual position and angle settings



BPM Applications V: BBA & Reproducibility of Golden Orbit

courtesy of Michael Boege, PSI

- scan local bumps through each quadrupole
- variation of quadrupole strengths to minimize global rms orbit



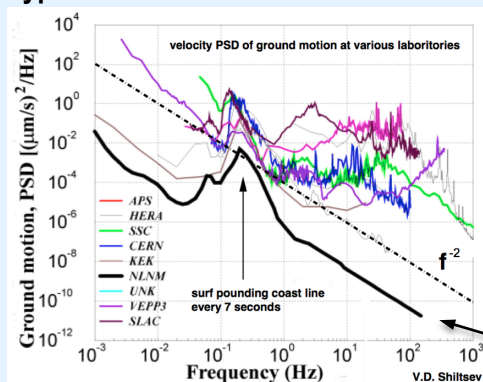
Beam Based Alignment

- ... aligns orbit to quadrupole axes
- ... accounts for mechanical & electrical BPM errors

BPM Applications VI: Global Fast Orbit Feedback & Short Term Stability

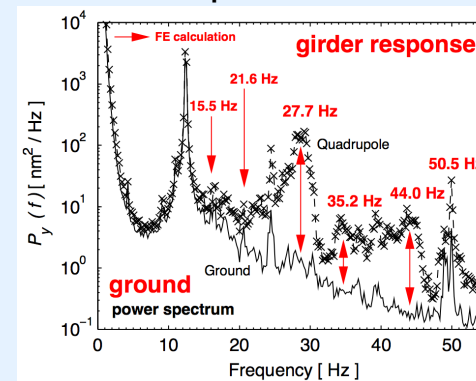
- ground motions below few hundred Hz typically define the short term stability at light sources
- amplification by girder response and beam optics cause disturbing beam motions for the users

Typical PSDs due to Ground Motion



lowest observed
seismic noise levels

SLS Girder Response to Ground Motion



courtesy of
Michael Boege, PSI

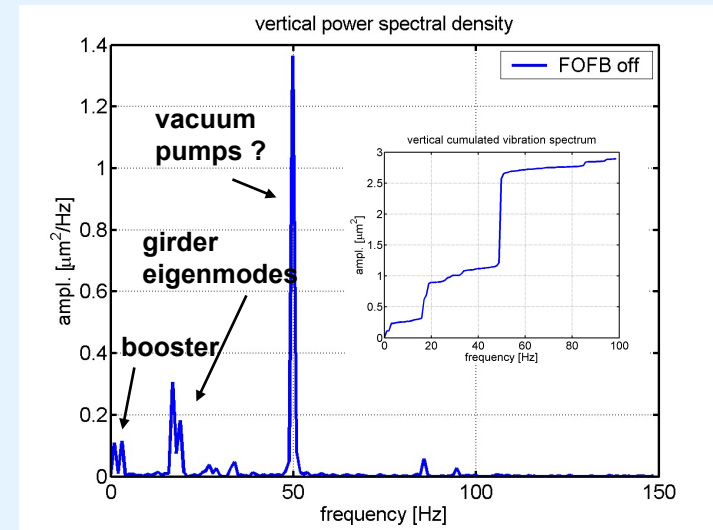
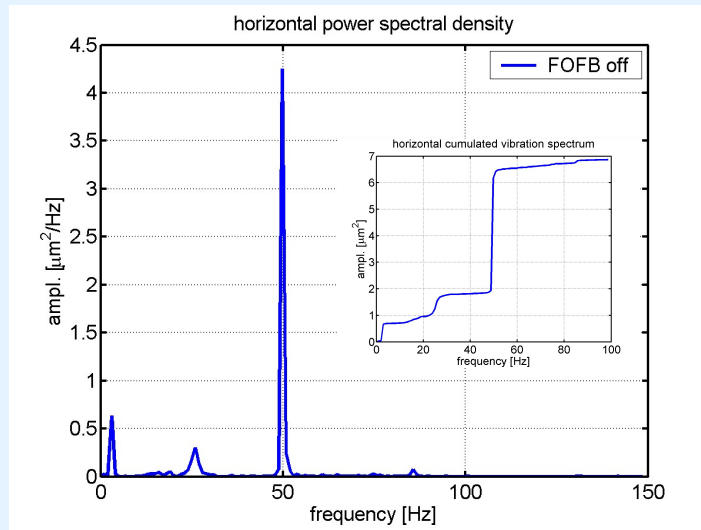
global fast orbit feedback system (FOFB) stabilizes electron beam to the „golden orbit“

Ingredients of Global Fast Orbit Feedbacks

- BPM data acquisition rate of a few (typically 10) kHz with only a few hundred nm integrated noise
- low noise corrector magnet power supplies with a few kHz bandwidth
- a centralized or distributed fast data distribution network for BPMs and corrector magnets
- calculation of orbit corrections through SVD or matrix inversion
- feedback loop is closed by (digitally implemented) PID controller

BPM Applications VII: Global Fast Orbit Feedback & Short Term Stability

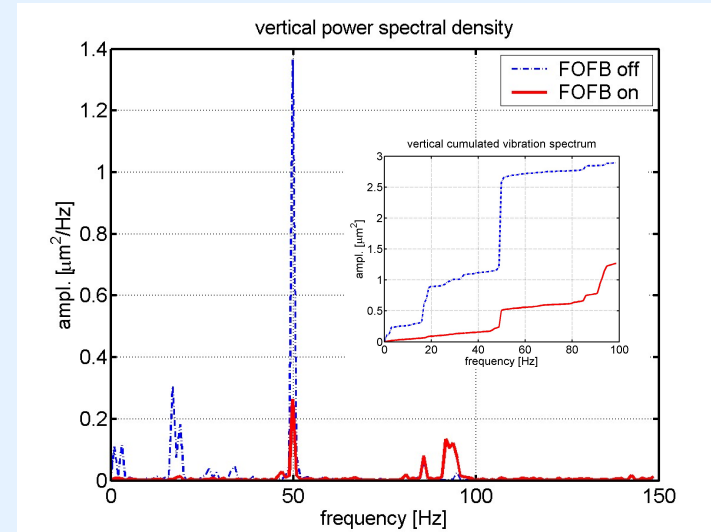
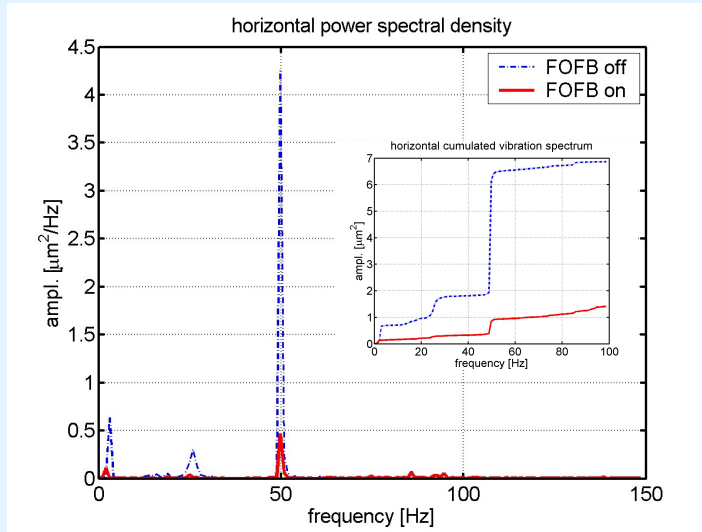
SLS Global Orbit Distortions without Fast Orbit Feedback



- measured at tune BPM outside of feedback loop ($\beta_x = 11 \text{ m}$, $\beta_y = 18 \text{ m}$)
- no ID-gap changes

BPM Applications VII: Global Fast Orbit Feedback & Short Term Stability

Performance of SLS Global Fast Orbit Feedback



- measured at tune BPM outside of feedback loop ($\beta_x = 11 \text{ m}$, $\beta_y = 18 \text{ m}$)
- no ID-gap changes

FOFB – Accumulated Power Densities (1 – 150 Hz)

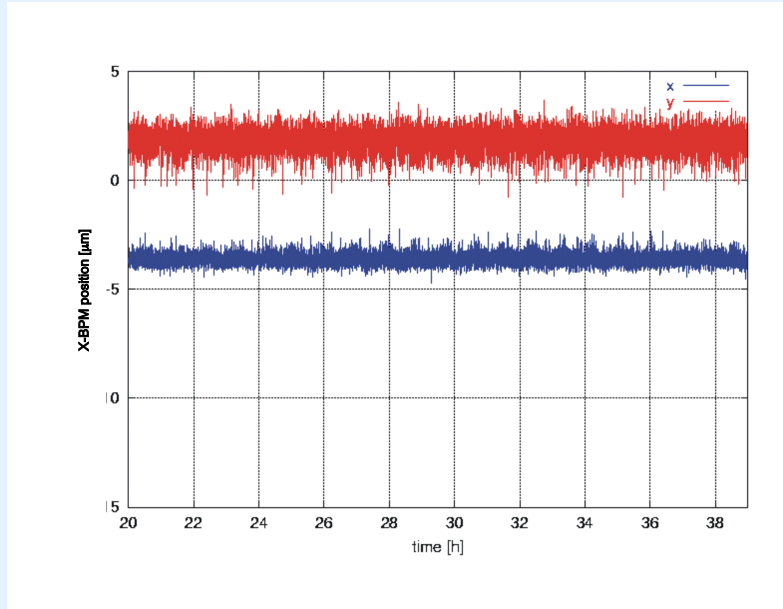
FOFB	horizontal		vertical	
	off	on	off	on
1- 100 Hz	$0.83 \mu\text{m} \cdot \sqrt{\beta_x}$	$0.38 \mu\text{m} \cdot \sqrt{\beta_x}$	$0.40 \mu\text{m} \cdot \sqrt{\beta_y}$	$0.27 \mu\text{m} \cdot \sqrt{\beta_y}$
100-150 Hz	$0.08 \mu\text{m} \cdot \sqrt{\beta_x}$	$0.17 \mu\text{m} \cdot \sqrt{\beta_x}$	$0.06 \mu\text{m} \cdot \sqrt{\beta_y}$	$0.11 \mu\text{m} \cdot \sqrt{\beta_y}$
1-150 Hz	$0.83 \mu\text{m} \cdot \sqrt{\beta_x}$	$0.41 \mu\text{m} \cdot \sqrt{\beta_x}$	$0.41 \mu\text{m} \cdot \sqrt{\beta_y}$	$0.29 \mu\text{m} \cdot \sqrt{\beta_y}$

Examples (1 – 150 Hz):

- tune BPM ($\beta_y = 18 \text{ m}$): $\sigma_y = 1.2 \mu\text{m}$
- ID 6S ($\beta_y = 0.9 \text{ m}$): $\sigma_y = 0.28 \mu\text{m}$

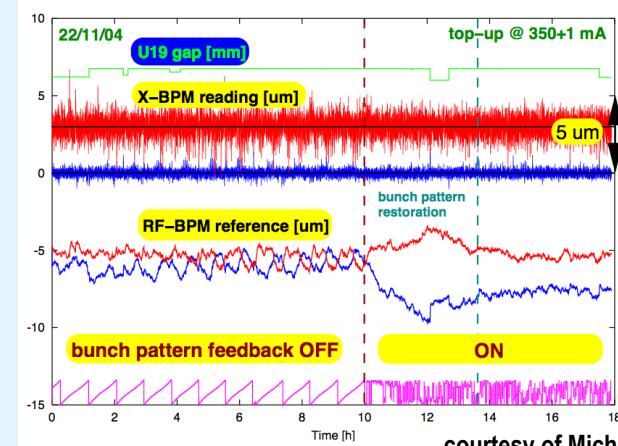
Photon BPMs: FOFB „Watchdog“ Function and Slow ID Feedbacks

Example of Photon Beam Stability at SLS Beamlines



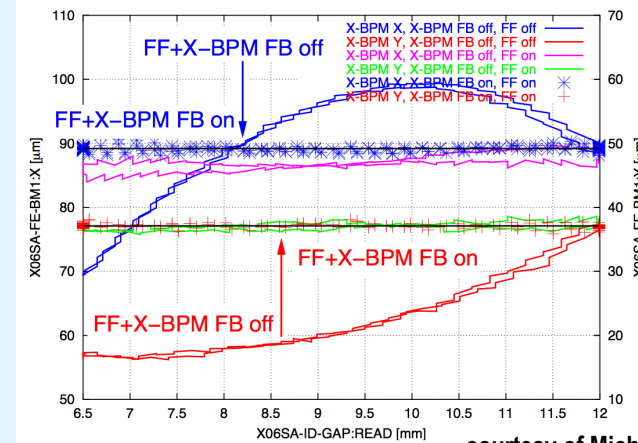
- systematic **electron BPM** effects are suppressed by slow, high level feedbacks on **photon BPM** readings
- resulting **photon beam stability** at the location of first optical elements of beamlines **< 1 µm** !

Photon BPM Stability vs. E-BPM Systematic Effects



courtesy of Michael Boege, PSI

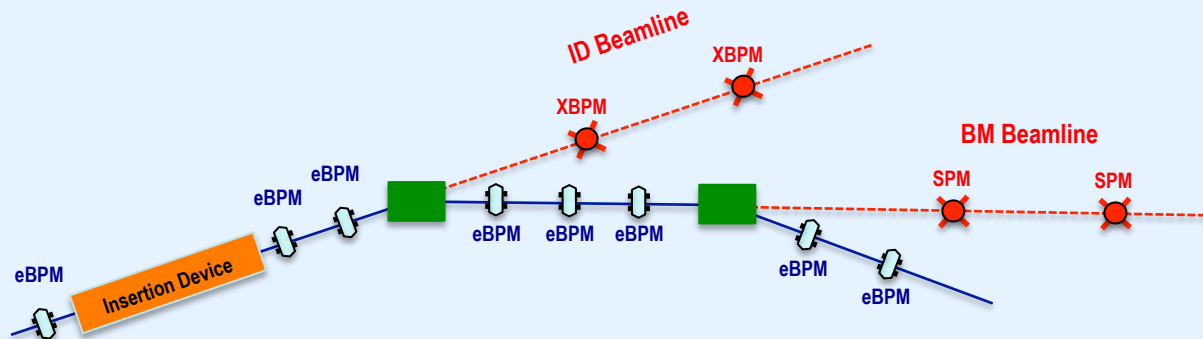
Photon BPM FB and Undulator Gap Variations



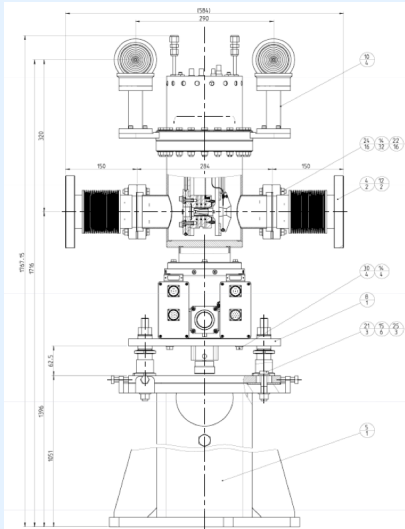
courtesy of Michael Boege, PSI

Photon BPMs: Front End Layout & BESS – FMB Blade Monitor Design

Photon BPM Layout with SPMs and XBPMs in Beamline Front Ends



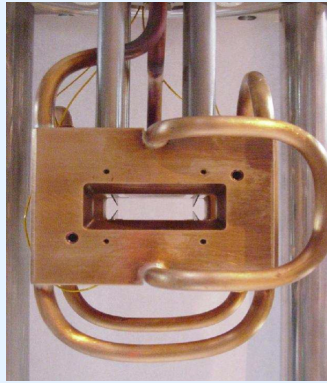
BESSY – FMB-Berlin Photon BPM Design



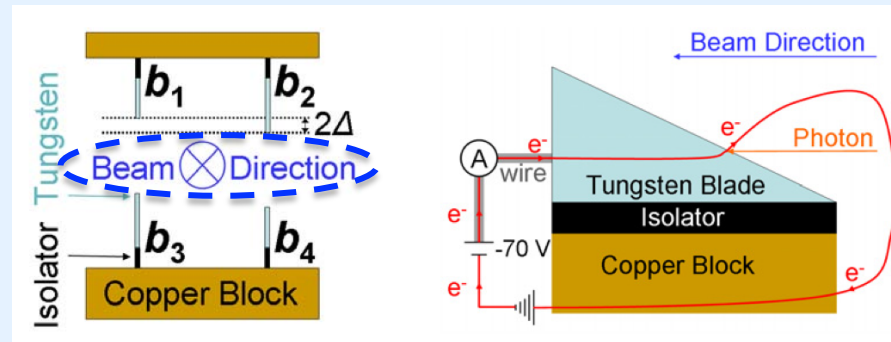
- **photon BPMs** provide better position resolution than **electron BPMs** due to larger lever arm
- absolute position reference to **photon BPM** alignment accuracy
- **photon BPM** FB compensates **electron beam** motions due undulator gap variations
- “out-of-loop” reference for global FOFB

Photon BPMs: Principle of SPM & XBPM Blade Monitors

„Staggered Pair“ Blade Monitors for Wiggler & Bending Magnet Beamlines



Schematic of SPM Arrangement for Wiggler & Bending Magnets

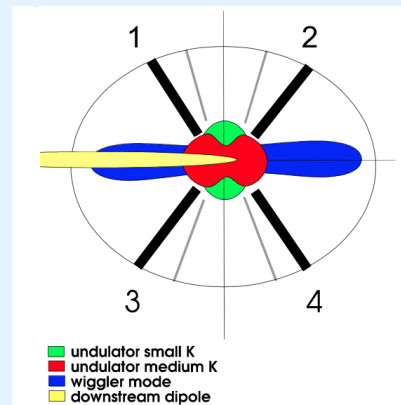


Vertical Photon Beam Position

$$P_v = \frac{\left(\frac{b_1 - b_3}{b_1 + b_3} \right) + \left(\frac{b_2 - b_4}{b_2 + b_4} \right)}{\left(\frac{b_1 - b_3}{b_1 + b_3} \right) - \left(\frac{b_2 - b_4}{b_2 + b_4} \right)} \cdot \Delta$$

with $2\Delta =$ blade offset

X-Ray BPM Blade Monitors for Undulator Beamlines



Position Determination (like e-BPMs)

$$X_{pos} = K_x \cdot \frac{(I_1 + I_3) - (I_2 + I_4)}{I_1 + I_2 + I_3 + I_4}$$

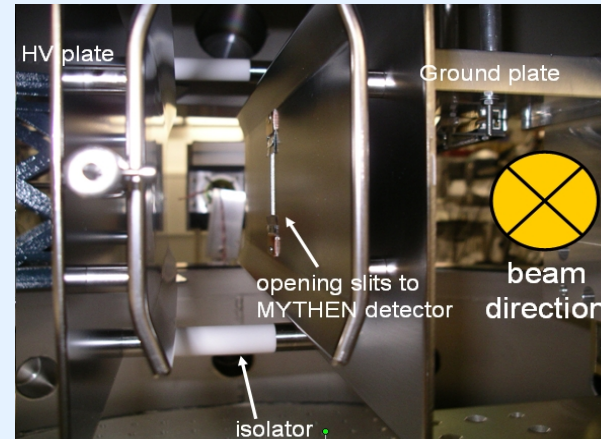
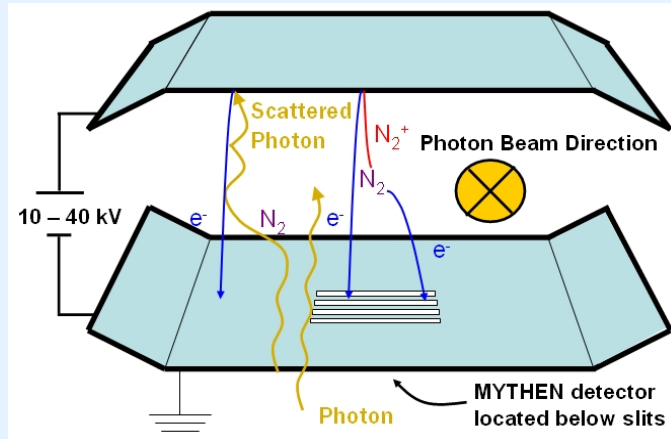
$$Y_{pos} = K_y \cdot \frac{(I_1 + I_2) - (I_3 + I_4)}{I_1 + I_2 + I_3 + I_4}$$

calibration required: SR contaminations from bends
optical mode / gap changes

Photo-induced currents (typ. nA – μA) are read out by low noise current amplifier & digitized for position processing

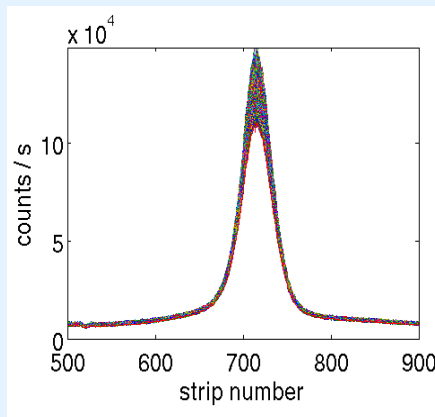
Gas Monitors – Example of Alternative Photon BPM for Light Sources

PSI Development of MYTHEN-based Gas Photon Monitor *

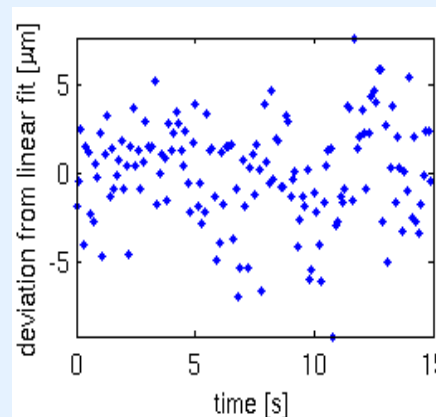


* courtesy of Thomas Wehrli, PSI

Photon Beam Profile °



Photon Beam Position °



Preliminary Results from SLS *

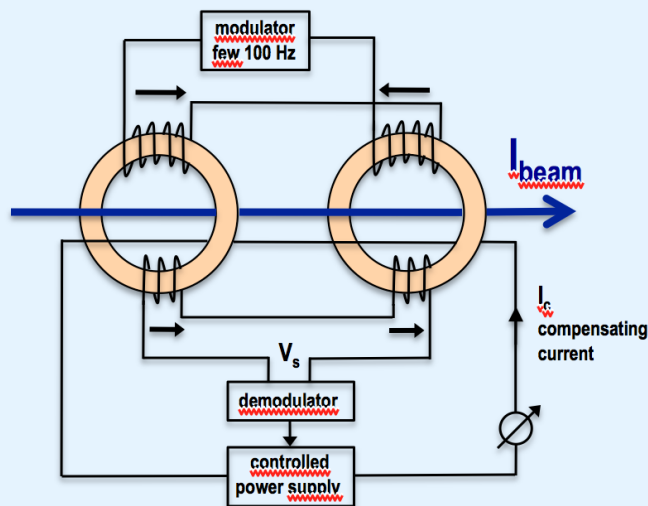
- position resolution: $\Delta x, y_{ph} = 2.9 \mu\text{m (rms)}$
- profile resolution: $\sigma_{ph} = 4.4 \mu\text{m}$
- resolutions are close to statistical limit
- photo-ions promise improvement of profile resolution by $\sqrt{\text{mass}}$
- integrating EIGER detector for SwissFEL

° photo-electrons @ 17 kV, $3.3 \cdot 10^{-6}$ mbar N_2 , 100 ms integration time

Beam Current Measurement: DC Parametric Current Transformer

Principle of the DC Parametric Current Transformer (introduced by K. Unser, CERN 1966):

- a modulator sends a current (few 100 Hz) through two coils, which are excited in opposite directions
- the pick-up coils are connected in series so that the resulting voltage (sum signal) V_s is zero
- a **beam current** I_{beam} induces a bias in the cores, so that V_s becomes non-zero and a 2nd harmonic of the modulator frequency will appear, which is converted to DC by the demodulator
- a compensating current I_c , which cancels the **beam current** I_{beam} is sent through the windings
- the measurement of I_c which corresponds to the **beam current** I_{beam} is done with a precision resistor



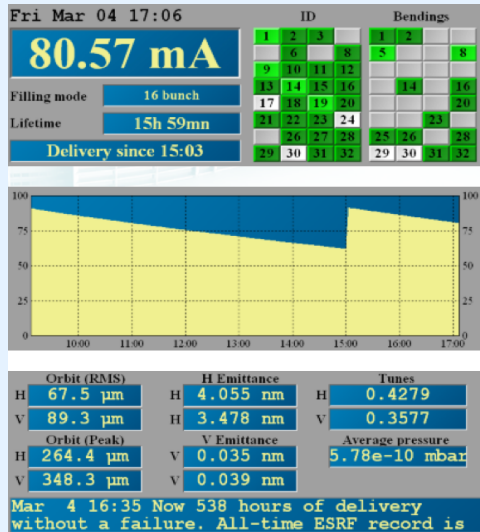
Commercially available NPCT from Bergoz Instrumentation



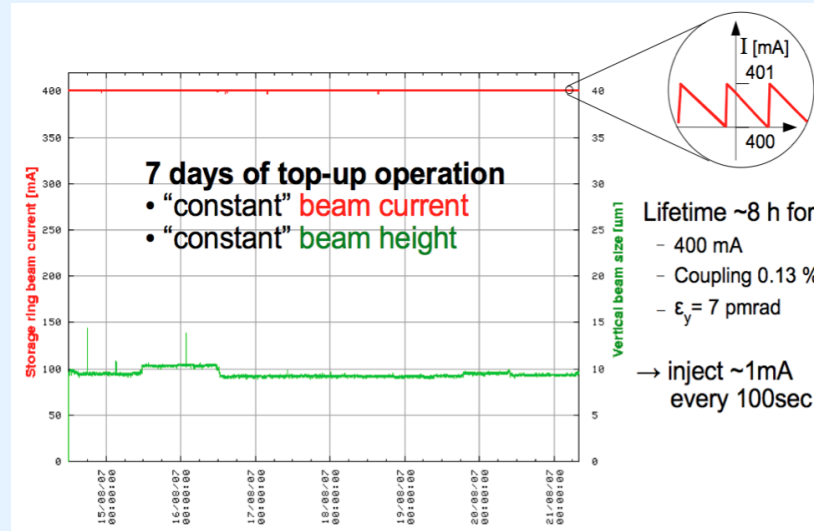
- resolution of $1 \mu\text{A} \rightarrow 10^{-5}$ of stored beam currents
- careful magnetic shielding and temperature control necessary

Beam Current Measurement: Injection Rate & Beam Lifetime

ESRF Status – Beam Current



SLS Top-Up Operation



→ precise beam current measurement provides...:

... Injection Rate: $I(t) = I_0 \cdot \dot{I}t$

... Beam Lifetime: $\frac{1}{\tau} = \frac{1}{\tau_{quantum}} + \frac{1}{\tau_{Touschek}} + \frac{1}{\tau_{elastic}} + \frac{1}{\tau_{inelastic}}$

$\tau_{quantum}$ particle losses due to quantum emission and radiation damping

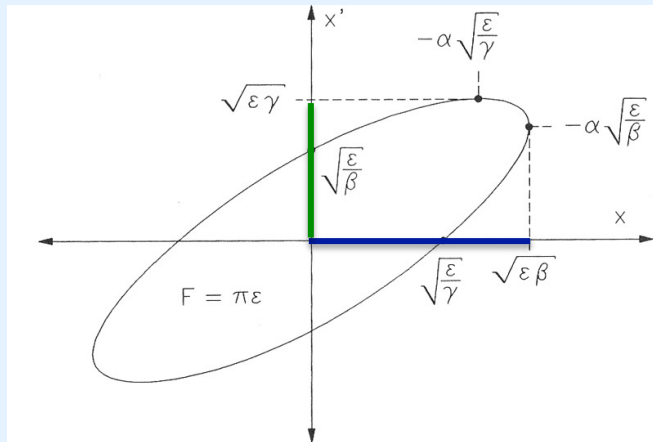
$\tau_{Touschek}$ particle losses due to elastic collisions of electrons in bunch

$\tau_{elastic}$ particle losses due to elastic scattering with residual gas molecules

$\tau_{inelastic}$ particle losses due to inelastic scattering → photo-emission / Bremsstrahlung

Synchrotron Radiation Monitors: Transverse Profiles and Emittance

beam emittance: projected area of transverse phase space volume



in case of a „flat lattice“ (low coupling) with $\eta_y \approx 0$

→ **horiz. beam size** $\sigma_x = \sqrt{\beta_x \varepsilon_x + (\sigma_\delta \eta_x)^2}$

use location with $\eta_x = 0$ for ε_x measurement

→ **vertical beam size** $\sigma_y = \sqrt{\beta_y \varepsilon_y}$

→ **beam divergence** $\sigma' = \sqrt{\gamma \varepsilon}$

- β -functions and dispersion are well known in light sources → ε can be determined from **beam size σ**
- synchrotron radiation from bending magnets (undulators and wigglers) are non-invasive sources
- small opening angle $\Theta \sim 1/\gamma$ (typ. $\ll 1$ mrad) of synchrotron radiation limits spatial resolution due to diffraction
→ spatial resolution limit: $\Delta \sigma \approx \lambda/2 \Delta \Theta \approx 250 \mu\text{m}$ for $\lambda = 500 \text{ nm}$ and $\Delta \Theta = 1 \text{ mrad}$

measurement of small beam sizes...:

- **X-ray pinhole camera**
- **interferometric techniques (UV, visible radiation)**
- **X-ray (VUV) imaging**

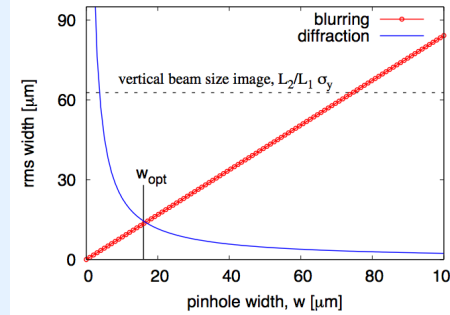
Synchrotron Radiation Monitors: X-Ray Pinhole Camera

X-ray pinhole camera resolution is limited by:

... blurring
$$\sigma_{blurr} = \frac{w(L_1 + L_2)}{\sqrt{12} \cdot L_1}$$

... diffraction
$$\sigma_{diff} = \left(\frac{\sqrt{12}}{4\pi} \right) \frac{\lambda L_2}{w}$$

Example from ALBA, U. Iriso et al., EPAC 2006

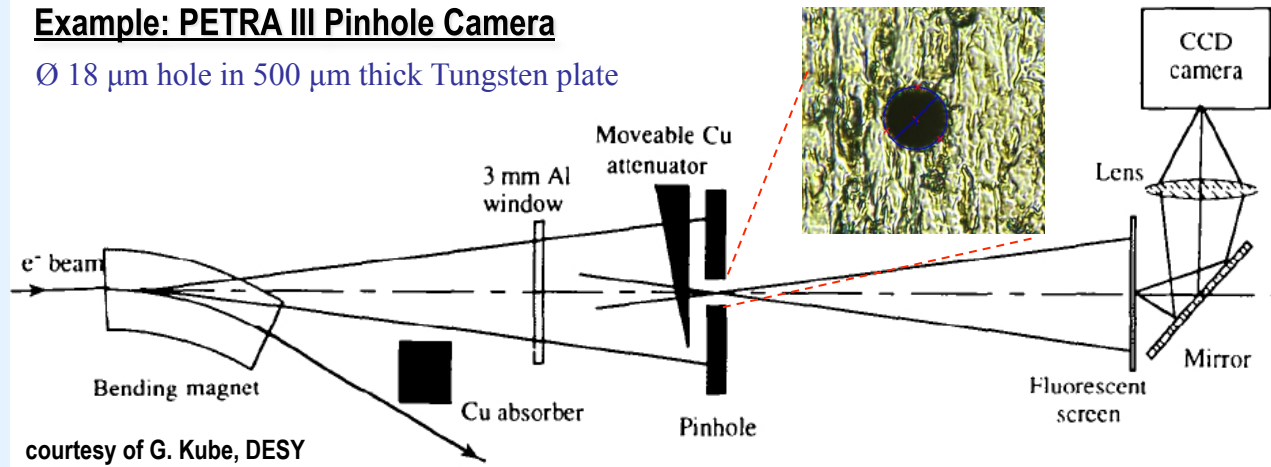


with $L_1 = 6 \text{ m}$
 $L_2 = 12 \text{ m}$
 $\lambda = 12 \text{ nm (17 keV)}$
 $\rightarrow w = 20 \text{ μm}$

typical resolution limitation of x-ray pinhole cameras ~ 10 μm

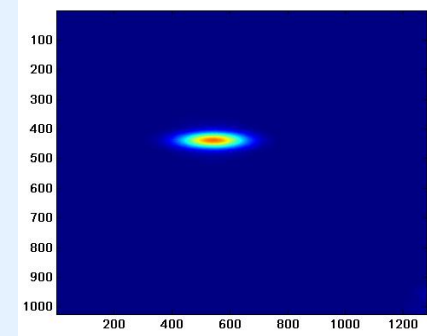
Example: PETRA III Pinhole Camera

Ø 18 μm hole in 500 μm thick Tungsten plate



courtesy of G. Kube, DESY

ESRF ID-25 X-Ray Pinhole Camera

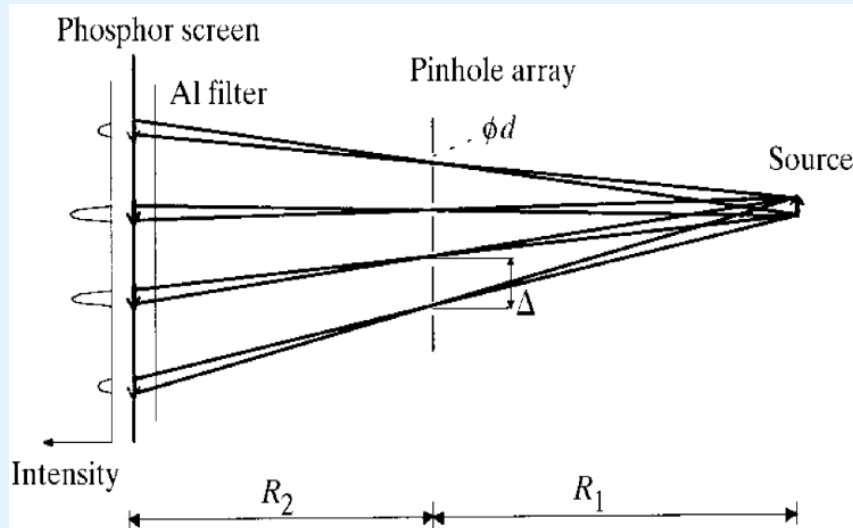


courtesy of K.Scheidt, ESRF

P.Elleaume, C.Fortgang, C.Penel and E.Tarazona, J.Synchrotron Rad. 2 (1995) , 209

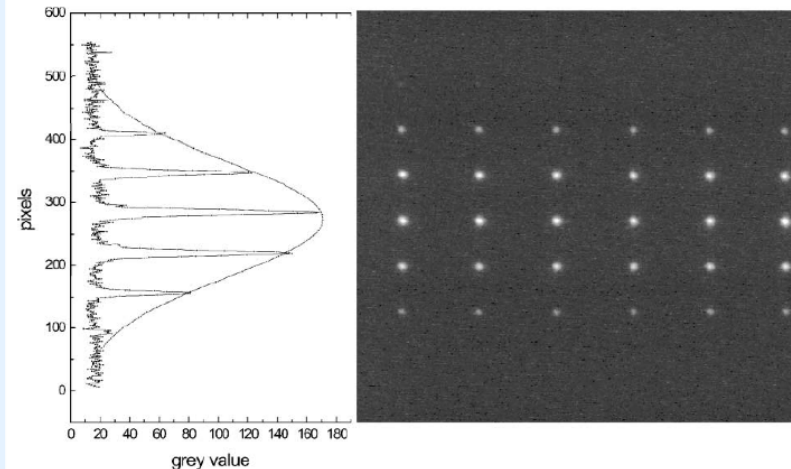
Synchrotron Radiation Monitors: X-Ray Pinhole Array

BESSY II X-Ray Pinhole Array



W.B. Peatman, K. Holldack, J. Synchrotron Rad. (1998) 5, 639-641

K. Holldack et al. / Nuclear Instruments and Methods in Physics Research A 467-468 (2001) 235-238



diffraction limited resolution: $\sim 11 \mu\text{m}$

- simultaneous measurement of...: → **beam size** through single pinhole image
 → **beam divergence** through envelope

Synchrotron Radiation Monitors: Principle of Interference Monitors

a **two-beam (double-slit) Michelson-type interferometer** adapted from stellar interferometry by T. Mitsuhashi

→ beam size is estimated from the visibility of interferogram, indicating the degree of complex coherence

van Cittert-Zernike's theorem

relates a **transverse distribution $f(y)$** of an object with the **degree of spatial coherence $\gamma(y)$** via Fourier Transform:

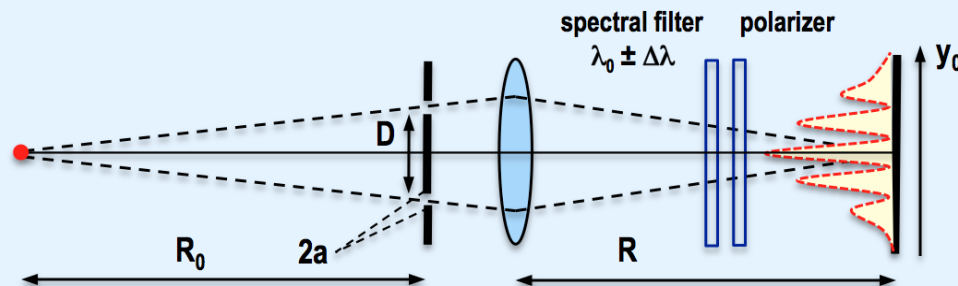
$$\gamma(\nu) = \int f(y) \exp(-i2\pi \nu y) dy \quad \text{with spatial frequency} \quad \nu = \frac{D}{\lambda R_0}$$

intensity of interference pattern is given by:
$$I(y_0) = I_0 \left[\text{sinc} \left(\frac{2\pi a}{\lambda R} y_0 \right) \right] \cdot \left[1 + |\gamma| \cos \left(\frac{2\pi D}{\lambda R} y_0 + \phi \right) \right]$$

and the **fringe visibility γ** is related to the **rms width of the interference pattern σ_D** by:
$$\gamma = \exp \left(-\frac{D^2}{2\sigma_D^2} \right)$$

→ **beam size** of an object is given by:

$$\sigma_y = \frac{\lambda R}{\pi D} \cdot \sqrt{\frac{1}{2} \ln \left(\frac{1}{\gamma} \right)}$$



Synchrotron Radiation Monitors: Principle of Interference Monitors

a two-beam (double-slit) Michelson-type interferometer adapted from stellar interferometry by T. Mitsuhashi

→ beam size is estimated from the visibility of interferogram, indicating the degree of complex coherence

van Cittert-Zernike's theorem

relates a transverse distribution $f(y)$ of an object with the degree of spatial coherence $\gamma(y)$ via Fourier Transform:

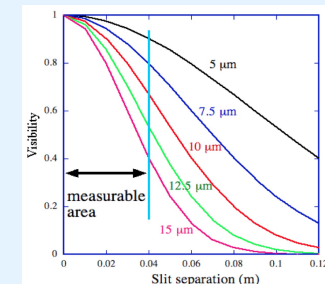
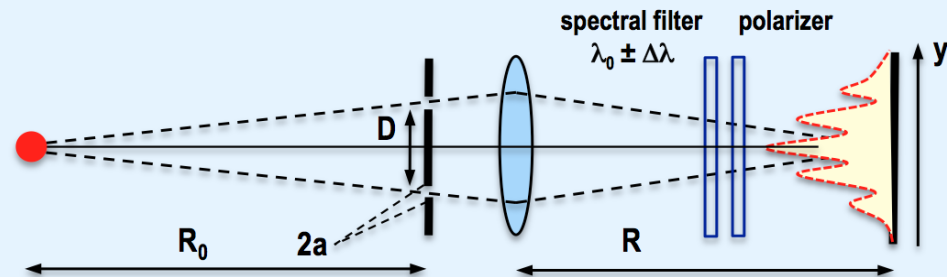
$$\gamma(\nu) = \int f(y) \exp(-i2\pi \nu y) dy \quad \text{with spatial frequency} \quad \nu = \frac{D}{\lambda R_0}$$

intensity of interference pattern is given by:
$$I(y_0) = I_0 \left[\text{sinc} \left(\frac{2\pi a}{\lambda R} y_0 \right) \right] \cdot \left[1 + |\gamma| \cos \left(\frac{2\pi D}{\lambda R} y_0 + \phi \right) \right]$$

and the fringe visibility γ is related to the rms width of the interference pattern σ_D by:
$$\gamma = \exp \left(-\frac{D^2}{2\sigma_D^2} \right)$$

→ beam size of an object is given by:

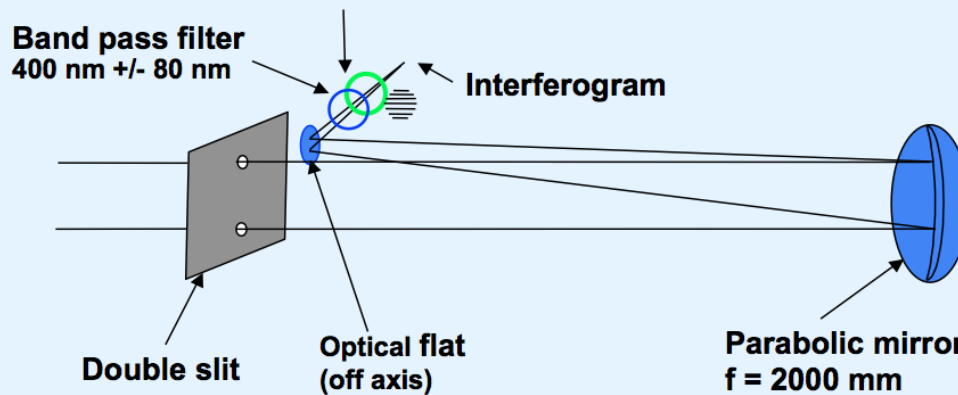
$$\sigma_y = \frac{\lambda R}{\pi D} \cdot \sqrt{\frac{1}{2} \ln \left(\frac{1}{\gamma} \right)}$$



Synchrotron Radiation Monitors: ATF Interference Monitor (with Mirror Optics)

T. Naito and T. Mitsuhashi, Phys. Rev. ST Accel. Beams 9 (2006) 122802

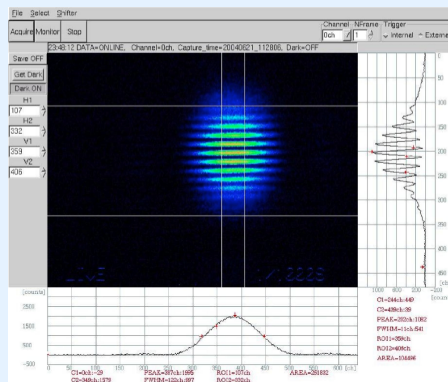
Schematic Set-Up of ATF Interference Beam Size Monitor



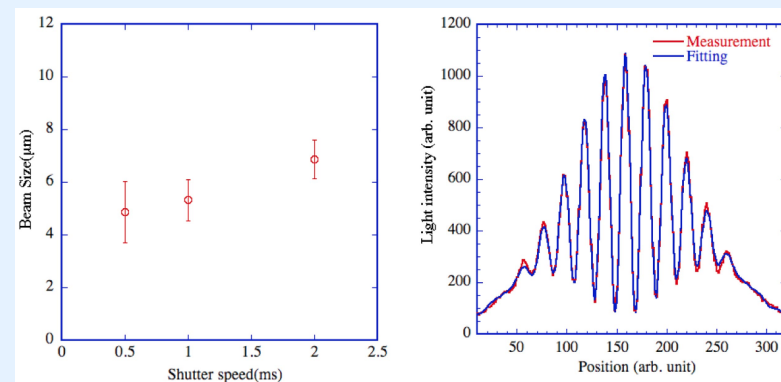
minimal measured beam size:

$$\sigma_y = 4.73 \pm 0.55 \mu\text{m}$$

Example of an Interferogram



Beam Size vs. Shutter Time and Fit of Interferogram



SR Monitors: Imaging of Vertically Polarized Optical Radiation

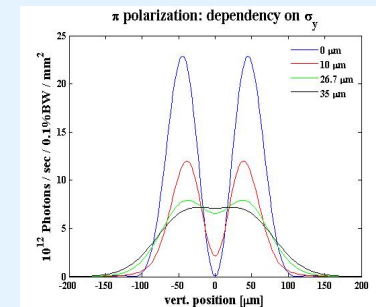
courtesy of Åke Andersson, MAX-lab

- for an ideally “flat beam” ($\sigma_y = 0$) → only horizontal polarization in the midplane
- vertical polarization only above and below the midplane

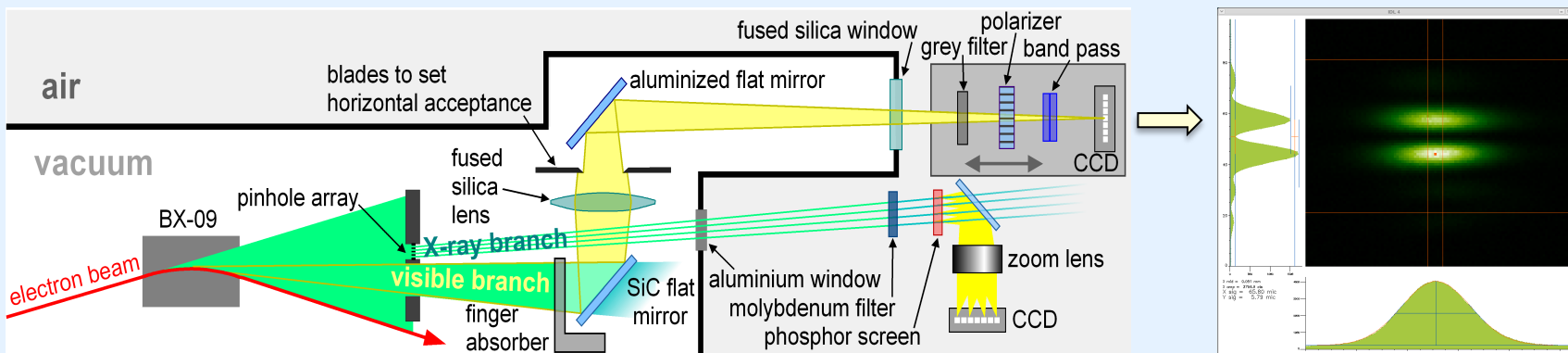
- for a “real beam” ($\sigma_y > 0$) → some vertical polarization can also be observed in the midplane

imaging vertically polarized SR in the visible

- two peaked distribution
- fringe visibility depends on vertical beam size σ_y



Schematic Set-Up of Visible Light SR Monitor at SLS



vertical beam size $\sigma_y = 5.8 \mu\text{m}$ for $\beta_y = 13.5 \text{ m}$ → vertical $\varepsilon_y = 2.5 \text{ pm}$ (natural limit from $1/\gamma$: $\varepsilon_{y,\text{min}} = 0.2 \text{ pm}$)

SR Monitors: Imaging with X-Ray (Focusing) Optics

Reflective Optics:

→ Kirkpatrick-Baez mirror scheme of grazing incidence ($\theta < 0.5^\circ$) with pair of ellipsoidal / cylindrical curved mirrors

Example: Advanced Light Source Diagnostics Beamline

T.R. Renner, H.A. Padmore, R. Keller, Rev.Sci.Instrum. 67 (1996) 3368

Diffraction Optics:

→ Fresnel Zone Plates: spacing of rings (e.g. Si, Au) result in constructive interference of light waves in focal point

Examples: X-Ray Beam Imager at Spring-8

S. Takano, M. Masaki, H. Ohkuma, Proc. DIPAC05, Lyon, France (2005) 241 and NIM A556 (2006) 357

Fresnel Zone Plate Monitor at ATF (KEK)

K. Ida et al., NIM A506 (2003) 49 and H. Sakai et al., Phys. Rev. ST Accel. Beams 10 (2007) 042801

Refractive Optics:

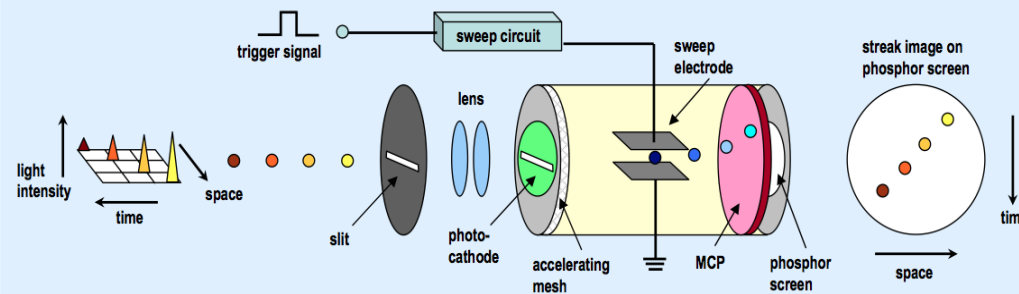
→ many (30 – 100) Compound Refractive Lenses made from Al or Be for focusing hard X-ray radiation (20 keV)

Example: PETRA III Diagnostics Beamline for Emittance Measurements

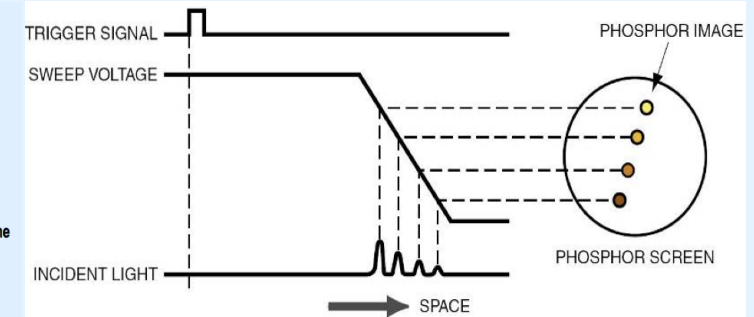
G. Kube et al., Proc. IPAC'10, Kyoto, Japan (2010), MOPD089, 909

Bunch Length Measurement with Visible SR: Streak Camera

Principle of Streak Camera Measurement



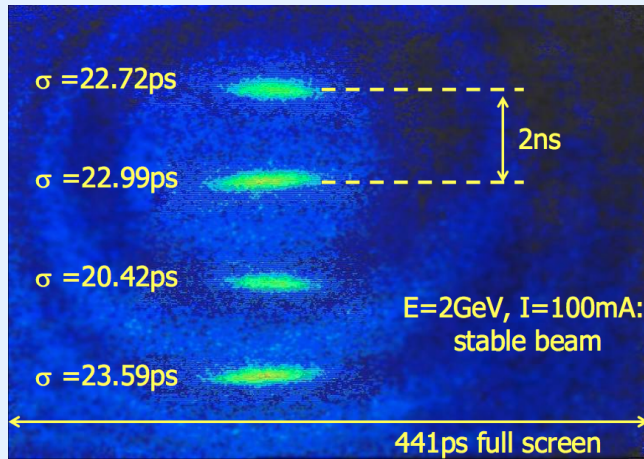
Streak Camera Timing Diagram



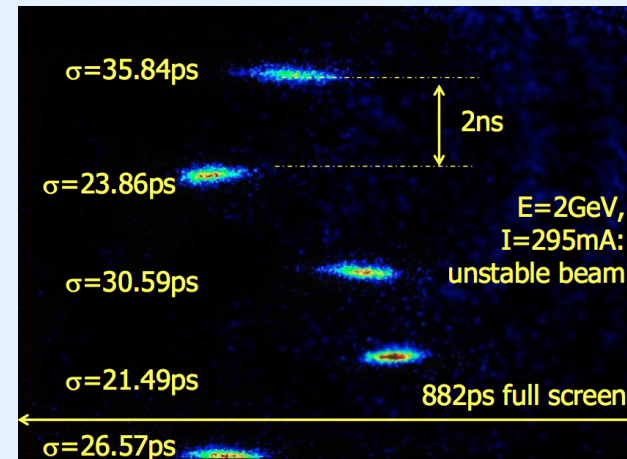
- visible light pulses from synchrotron radiation (bending magnet) are converted on the SC photo-cathode into a number of photo-electrons, which are proportional to the incident light distribution
- the photo-electrons are accelerated along the streak tube, transverse (vertically) swept by deflecting plates to convert the incident time distribution in a spatial distribution on the MCP
- the photo-electrons are amplified by the MCP and converted back to visible light on the phosphor screen
- an initial spatial offset of the light pulses at the entrance slit is preserved on the phosphor screen
- at synchrotron light sources „dual-sweep“ synchroscan streak cameras are typically used to observe electron bunch lengths along the storage ring filling pattern and / or during several turns around the storage ring

Examples of Synchroscan Streak Camera Measurements (by M. Ferianis, ELETTRA)

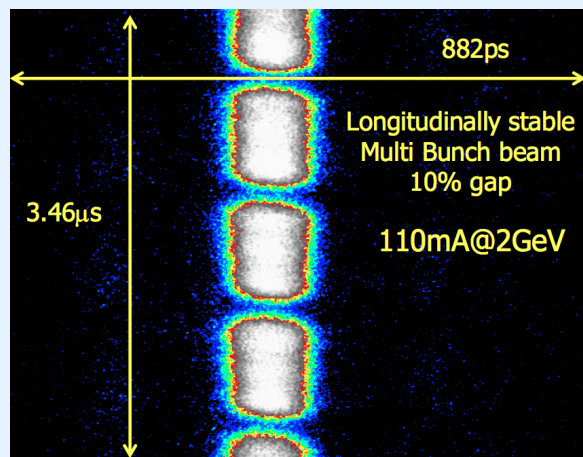
Four Bunch Mode – Stable Beam



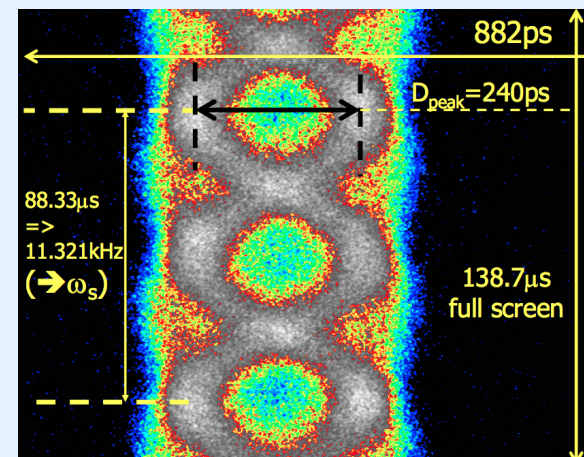
Four Bunch Mode – Unstable Beam



Multi-Bunch Mode – Stable Beam



Multi-Bunch Mode – Unstable Beam



Light Source Diagnostics – Summary (personal opinion...)

various **diagnostics devices** and **measurement examples** have been presented...

Electron BPMs....:

- key diagnostic for synchrotron light source
- turn-by-turn and high resolution (FOFB) measurement modes provide **tunes, chromaticity, β -functions (orbit response) and beam stability**

Photon BPMs....:

- provide higher resolution than electron BPMs but many systematic effects
- **“watch-dog” functionality for electron BPMs**
- **slow feedbacks to compensate undulator gap variations and systematic e-BPM effects**

Current Monitors....:

- high resolution DCCT allows current measurement at 10^{-5} level ($1 \mu\text{A}$)
- **determination of beam lifetime and injection efficiency (important for top-up operation)**

SR Monitors....:

- determine transverse emittances through measurement of (vertical) beam sizes
- bunch lengths, filling pattern and longitudinal stability with diodes or streak camera
- **application of pinhole camera, interference monitors and X-ray imaging**
- **use of visible light for bunch length and filling pattern**